

*Large fine-scale spatiotemporal variations of CH<sub>4</sub> diffusive fluxes from shrimp aquaculture ponds affected by organic matter supply and aeration in Southeast China*

Article

Accepted Version

Yang, P., Zhang, Y., Yang, H. ORCID: <https://orcid.org/0000-0001-9940-8273>, Zhang, Y., Xu, J., Tan, L., Tong, C. and Lai, D. Y. F. (2019) Large fine-scale spatiotemporal variations of CH<sub>4</sub> diffusive fluxes from shrimp aquaculture ponds affected by organic matter supply and aeration in Southeast China. *Journal of Geophysical Research: Biogeosciences*, 124 (5). pp. 1290-1307. ISSN 2169-8961 doi: <https://doi.org/10.1029/2019JG005025> Available at <https://centaur.reading.ac.uk/84289/>

It is advisable to refer to the publisher's version if you intend to cite from the work. See [Guidance on citing](#).

To link to this article DOI: <http://dx.doi.org/10.1029/2019JG005025>

Publisher: American Geophysical Union

including copyright law. Copyright and IPR is retained by the creators or other copyright holders. Terms and conditions for use of this material are defined in the [End User Agreement](#).

[www.reading.ac.uk/centaur](http://www.reading.ac.uk/centaur)

## **CentAUR**

Central Archive at the University of Reading

Reading's research outputs online

# Large fine-scale spatiotemporal variations of CH<sub>4</sub> diffusive fluxes from shrimp aquaculture ponds affected by organic matter supply and aeration in Southeast China

Ping Yang<sup>1,2,3‡</sup>, Yan Zhang<sup>1,2,3‡</sup>, Hong Yang<sup>4,5,6\*</sup>, Yifei Zhang<sup>1,2</sup>, Jin Xu<sup>2</sup>, Lishan Tan<sup>1,2</sup>, Chuan Tong<sup>1,2,3\*</sup>, Derrick Y.F. Lai<sup>7</sup>

<sup>1</sup>Key Laboratory of Humid Subtropical Eco-geographical Process of Ministry of Education, Fujian Normal University, Fuzhou 350007, P.R. China,

<sup>2</sup>School of Geographical Sciences, Fujian Normal University, Fuzhou 350007, P.R. China,

<sup>3</sup>Research Centre of Wetlands in Subtropical Region, Fujian Normal University, Fuzhou 350007, P.R. China,

<sup>4</sup>College of Environmental Science and Engineering, Fujian Normal University, Fuzhou, 350007, China,

<sup>5</sup>Collaborative Innovation Center of Atmospheric Environment and Equipment Technology, Jiangsu Key Laboratory of Atmospheric Environment Monitoring and Pollution Control, School of Environmental Science and Engineering, Nanjing University of Information Science & Technology, 219 Ningliu Road, Nanjing 210044, China,

<sup>6</sup>Department of Geography and Environmental Science, University of Reading, Reading, RG6 6AB, UK,

<sup>7</sup>Department of Geography and Resource Management, The Chinese University of Hong Kong, Shatin, New Territories, Hong Kong SAR, China

## \*Correspondence to:

H. Yang (hongyanghy@gmail.com, Telephone 0044(0)1183787750) or C. Tong (tongch@fjnu.edu.cn, Telephone 086-0591-87445659)

‡ Ping Yang and Yan Zhang contributed equally to this work.

**Abstract** Mariculture shrimp ponds are important CH<sub>4</sub> sources to the atmosphere. However, the spatiotemporal variations of CH<sub>4</sub> concentration and flux at fine spatial scales in mariculture ponds are poorly known, particularly in China, world largest aquaculture producer. In this study, the plot-scale spatiotemporal variations of water CH<sub>4</sub> concentration and flux, both within and among ponds, were researched in shrimp ponds in Shanyutan wetland, Min River Estuary, Southeast China. The average water CH<sub>4</sub> concentration and diffusion flux across the water-air interface in the shrimp ponds over the shrimp aquaculture period varied from  $2.29 \pm 0.29$  to  $50.48 \pm 20.91$   $\mu\text{M}$  and from  $0.09 \pm 0.01$  to  $2.32 \pm 0.95$   $\text{mmol m}^{-2} \text{h}^{-1}$ , respectively. The CH<sub>4</sub> emissions from the estuarine ponds varied greatly in seasonal dynamics, with peaks in August and September, which was similar to the trend of water temperature and dissolved oxygen (DO) concentrations. There was no remarkable difference in CH<sub>4</sub> concentration and flux between shrimp ponds, but significantly spatiotemporal differences in CH<sub>4</sub> concentration and flux within the ponds. Significantly higher emissions occurred in the feeding zone, accounting for approximately 60% of total CH<sub>4</sub> emission flux, while much lower CH<sub>4</sub> emissions appeared in aeration zone, contributing 14% to total flux. This study suggests the importance of considering spatiotemporal variation in the whole-pond estimates of CH<sub>4</sub> concentration and flux. In light of such high spatial variation within ponds, improving aeration and feed utilization efficiency would help to mitigate CH<sub>4</sub> emissions from mariculture ponds.

## 1. Introduction

Since the beginning of the industrial revolution, greenhouse gases (GHGs) emissions produced by human activities have increased markedly (IPCC, 2013). Methane (CH<sub>4</sub>) is an important greenhouse gas that has a much larger global warming potential than CO<sub>2</sub> and contributes to approximately 20% of global radiative forcing (IPCC, 2013). Global atmospheric CH<sub>4</sub> levels have increased from 0.7  $\mu$ atm in 1750 to 1.8  $\mu$ atm in 2015, exceeding the pre-industrial levels by about 150% (World Meteorological Organization, 2016). Worse, some projections indicate a further doubling by 2100 (Cotovicz Jr., et al., 2016; IPCC, 2013). Accurately quantifying CH<sub>4</sub> emission and concentration in various ecosystems provides an indispensable basis for predicting future CH<sub>4</sub> emissions and climate change.

Aquatic ecosystems (e.g., lakes, rivers, and reservoirs) actively process terrestrial carbon, and frequently supersaturated with CH<sub>4</sub> in most time (Blees et al., 2015; Diem et al., 2012; Wen et al., 2016; Yang & Flower, 2012). They are important sources to the global CH<sub>4</sub> budget (Bastviken et al., 2011; Tangen et al., 2016; Yang et al., 2011), and it was estimated that global inland waters emit 0.65 Pg of C (CO<sub>2</sub>-eq) year<sup>-1</sup> in the form of CH<sub>4</sub> (Bastviken et al., 2011). Due to the limitation of data (Bastviken et al., 2011), the CH<sub>4</sub> emissions from tropical rivers have been markedly underestimated (Borges et al., 2015). Furthermore, the accurate estimate of the regional and global CH<sub>4</sub> budgets remains challenging also because of overlooked the role of small ponds (Holgerson, 2015; Holgerson & Raymond, 2016; Long et al., 2016). As an indispensable part of the global small ponds, some recent studies have suggested that aquaculture ponds can be indispensable CH<sub>4</sub> emissions (Chen et al., 2016; Hu et al., 2012; Wu et al., 2018; Yang et al., 2015b; Yuan et al., 2019). As an important part of the global small ponds, some recent studies have suggested that aquaculture ponds are indispensable CH<sub>4</sub> emission sources (Chen et al., 2016; Hu et al., 2012; Wu et al., 2018; Yang et al., 2015b; Yuan et al., 2019). Although some efforts have been made on characterizing CH<sub>4</sub> fluxes in aquaculture ponds, the number of field records of CH<sub>4</sub> emissions from aquaculture ponds remains very scarce as compared to those from other aquatic systems (e.g., lakes and reservoirs) (Yang et al., 2018a). More importantly, the magnitude of spatial variation in CH<sub>4</sub> fluxes, both within pond and between nearby ponds, is poorly understood so far, and there is a lack of integrated analysis of both spatial and temporal variations. Furthermore, the dominant pathway of CH<sub>4</sub> release from aquaculture ponds into atmospheric environment remains poorly documented. Detailed field studies including both the spatial and temporal dimensions are critical to better understand the variation, and to develop more accurate approaches for upscaling to whole-pond CH<sub>4</sub> emissions and further large-scale assessments of pond CH<sub>4</sub> fluxes.

China has world's largest mariculture industry, contributing more than 17% of world's mariculture volume and approximately a third of global value in 2014 (FAO, 2017). Shrimp aquaculture is one of the most important mariculture productions in China and it is widely distributed in the subtropical estuaries along the coastal regions (Yang et al., 2017a). These mariculture ponds are highly heterogeneous over time and space

owing to variations in topography, environmental factors (e.g., temperature, nutrient levels, dissolved oxygen, and others), astronomical tidal levels and other factors (Yang et al., 2018a), which may in turn lead to large uncertainties in the emission of CH<sub>4</sub>. To improve the understanding of fine-scale spatiotemporal variation in CH<sub>4</sub> dynamics, and their implications for effectively upscaling pond fluxes to regional scales, this study researched fine-scale CH<sub>4</sub> flux dynamics across the water-atmosphere interface of shrimp ponds in Southeast China. The research aims are 1) to determine the spatial variations in CH<sub>4</sub> fluxes both within pond and among ponds; 2) to assess the seasonal dynamics of CH<sub>4</sub> flux in the shrimp ponds and main influencing factors; and 3) to determine the dominant pathway of CH<sub>4</sub> release from the shrimp ponds into atmospheric environment.

## 2. Materials and Methods

### 2.1. Study Area Description

This study was conducted within the central-western part of the Shanyutan wetland (26°00'36"–26°03'42"N, 119°34'12"–119°40'40"E) located in the Min River estuary (MRE) in Southeast China (Figure 1). Climate in the region is characterized by warm and wet, with a mean annual temperature of 19.6°C and a mean annual precipitation of 1350 mm (Tong et al., 2010). The tides at the wetland are typically semidiurnal, with an average range of approximately 4.5 m. The average salinity of tidal water in the Min River estuary is 4.2±2.5‰. The dominant vegetation species of the Shanyutan wetland include the native *Cyperus malaccensis* and *Phragmites australis* and the invasive *Spartina alterniflora* (smooth cordgrass). Conversion of the tidal marsh ecosystem was performed in the Shanyutan wetland of the Min River estuary in recent years, and almost all of the converted lands were used for aquaculture (Yang et al., 2017a).

### 2.2. Shrimp Pond System and Management

Shrimp pond is one of the dominant landscapes in the Min River estuary. Most of the ponds were converted by the complete removal of original marsh vegetation. The aquaculture period usually starts in June and ends in November, with only one single crop of shrimps being produced each year (Yang et al., 2017b). Prior to shrimp production, these ponds were filled with salt water from an adjacent estuary using a submerged pump. The water depth in these shrimp ponds ranged between 1.1 and 1.8 m during the culture period. There was no water exchange during the farming period. The shrimps were fed with commercial aquatic feed pellets containing 42% protein (Yuehai™, Guangzhou, China) twice per day at 07:00 AM and 16:00 PM (local standard time), respectively, by direct application from a small boat. In each pond, three to five 1500 W paddlewheel aerators were operated four times in 07:00–09:00, 12:00–14:00, 18:00–20:00, and 00:00–03:00 (local standard time) to improve oxygen supply. Further details about the shrimp pond system and the associated management practices can be found in Yang et al. (2017b) and Yang et al. (2018a).

The pond is divided into three zones according to microtopography feature, water depth, and management practices (Figure 1c). Zone N is a nearshore area and inhabited by the tiny minority of submerged vegetation. Zone F is a deepwater area

(ditch) used for bait feeding and it is the major area for foraging, habitating and metabolic activity of shrimps. Zone A is a shallow area (platform) used for aeration activities, and to improve ponds oxygen supply. Water depth in Zone N typically 0.3–0.5 m, for Zone F (ditch) 1.5–1.8 m, and for Zone A (platform) 0.8–1.2 m. More details about the three zones of shrimp pond can be found in [Zhang et al. \(2019\)](#). To assess the plot-scale spatiotemporal variation of CH<sub>4</sub> emission from shrimp aquaculture ponds, water, sediment, and gas samples were collected from three commercial shrimp ponds in Shanyutan Wetland of the MRE ([Figure 1](#)), respectively. Basic characteristics about the selected shrimp ponds in the estuary are given in [Zhang et al. \(2019\)](#).

### 2.3. Measurement of the CH<sub>4</sub> Concentration and Flux

#### 2.3.1. CH<sub>4</sub> Concentration

Three transects were chosen in each pond for the measurement of water dissolved CH<sub>4</sub> concentration. Taking into account the shrimp grow-out cycle as well as the logistical feasibility of sampling in the shrimp farms, water samples from the shrimp ponds were collected in June and November 2017. At each pond, three sampling sites were deployed on a transect from the nearshore zone to the aeration zone in each pond (zones N, F, and A) ([Figure 1c](#)). Each whole-pond survey was completed between 10:00 and 16:00 (local standard time). Water samples for the determination of dissolved CH<sub>4</sub> concentration were collected in 55 mL pre-weighted serum glass bottles with silicone tubing, left to overflow, poisoned with a saturated solution of HgCl<sub>2</sub> (0.2 mL<sup>-1</sup>), sealed with a butyl stopper, and crimped with an aluminum cap ([Abril et al., 2007](#); [Borges et al., 2017](#); [Cotovicz Jr., et al., 2016](#)). CH<sub>4</sub> concentration was determined using the headspace technique and a gas chromatograph. Ultrahigh purity N<sub>2</sub> gas (99.999%) was injected into the glass bottle to create a 25 mL headspace. The N<sub>2</sub> gas entered the bottle via a syringe inserted in the rubber stopper at a slight positive pressure of 50 hPa, and 25 mL of water was pushed out of the bottle via a second syringe inserted in the stopper ([Xiao et al., 2017](#)). The samples were vigorously shaken to obtain complete equilibration between air and water phases ([Cotovicz Jr., et al., 2016](#)). After waiting for 0.5 h, the headspace CH<sub>4</sub> concentrations were determined using gas chromatography (GC-2010, Shimadzu, Kyoto, Japan) with flame ionization detection (FID). Five different concentrations of standard CH<sub>4</sub> gas, namely 2, 8, 500, 1000 and 10000 ppm, were used to calibrate the FID of gas chromatograph. The detection limits for CH<sub>4</sub> were 0.3 ppm, and the relative standard deviations of CH<sub>4</sub> analyses were  $\leq 2.0\%$  in 24 h. The dissolved CH<sub>4</sub> concentration *in situ* surface water was calculated according to a temperature and salinity-dependent Henry's law constant and accounted for CH<sub>4</sub> in the headspace and in the water ([Farías et al., 2017](#); [Wanninkhof, 1992](#); [Xiao et al., 2017](#)).

#### 2.3.2. CH<sub>4</sub> Flux from the Transfer Coefficient Method

Transfer coefficient method (Eq.1) was used to quantify the diffusive CH<sub>4</sub> flux ( $F_{m,d}$ , mmol m<sup>-2</sup> h<sup>-1</sup>) across the water-atmosphere interface at three transects across the ponds and in different months of the aquaculture period.

$$F_{m,d} = k(C_w - C_{eq}) \quad (1)$$

where  $k$  is the gas exchange velocity ( $\text{cm h}^{-1}$ ),  $C_w$  is the measured surface water (here at the depth 20 cm) dissolved  $\text{CH}_4$  concentration ( $\text{mmol L}^{-1}$ ), and  $C_{eq}$  is the equilibrium dissolved  $\text{CH}_4$  concentration relative to the atmospheric concentration at the prevailing *in situ* conditions ( $\text{mmol L}^{-1}$ ). The gas transfer coefficient  $k$  is dependent on wind speed and is normalized to a Schmidt number of 600 (Jahne et al., 1987; MacIntyre et al., 1995; Xiao et al., 2017). The wind speed was collected from the automatic weather station of the Min River Estuary Ecological Station in the Shanyutan wetland.  $k$  values were obtained from the model described by Cole & Caraco (1998) due to that their experiment environment (considering the influence of varying wind speeds on the estimate of  $k$  value) were closest to the studied shrimp ponds.

### 2.3.3. $\text{CH}_4$ Flux from Direct Measurement Using Chamber

In order to evaluate the potential role of  $\text{CH}_4$  ebullition flux from the shrimp ponds, total  $\text{CH}_4$  fluxes were determined by floating chamber. On each sampling date, three plastic floating chambers were deployed on transects L1 from the nearshore zone to the aeration zone of each pond. Chambers were with an area of  $0.1 \text{ m}^2$  and a volume of 5.2 L, and they were fitted with Styrofoam floats on their sides. They were covered with aluminum tape to minimize internal heating by sunlight. More details about the floating chambers can be found in Natchimuthu et al. (2016, 2017). Two air samples inside the chamber headspace were collected began at 9:00–11:00 AM on the 1<sup>st</sup> day and ended at the same time on the 2<sup>nd</sup> day over a 24 h period from chamber enclosure by using 60 mL plastic syringes equipped with three-way stopcocks. The samples were then immediately transferred to pre-evacuated airtight gas sampling bags (Dalian Delin Gas Packing Co., Ltd., China), transported to the laboratory, and analyzed using a gas chromatograph (GC-2010, Shimadzu, Kyoto, Japan) equipped with a FID within 24 h after sampling. The gas flux ( $F_{m, t}$ ,  $\text{mmol m}^{-2} \text{ h}^{-1}$ ) was calculated with the following Equation (2):

$$F_{m, t} = \frac{dn}{dt} \times \frac{1}{A} \quad (2)$$

where  $dn/dt$  is the slope of the amount of substance for  $\text{CH}_4$  over the sampling period ( $\text{mol h}^{-1}$ ) and  $A$  is the chamber area ( $\text{m}^2$ ). The amounts of  $\text{CH}_4$  in the chamber at different times were calculated using Equation (3):

$$n = (C_{\text{end}} - C_{\text{init}}) \times 10^{-6} \times \frac{P_{\text{tot}} \times V}{R \times T} \quad (3)$$

where  $C_{\text{init}}$  and  $C_{\text{end}}$  are respectively the initial and end concentration of  $\text{CH}_4$  across the water-air interface (ppm) (usually comes from GC measurement);  $P_{\text{tot}}$  is the total air pressure (usually  $\sim 1 \text{ atm} = 1013.15 \text{ hPa}$ );  $V$  is the chamber volume (L);  $R$  is the common gas constant ( $0.082056 \text{ L atm K}^{-1} \text{ mol}^{-1}$ ); and  $T$  is the absolute temperature during the gas sampling (K). Since chambers showed distinct nonlinear increases in methane concentration, this research considered the chambers captured the flux to the atmosphere including both flux by diffusion and by ebullition (bubble flux) from the shrimp ponds. Therefore, same as previous studies (Bastviken et al., 2004; Chuang et al., 2017; Keller & Stallard, 1994; Miller & Oremland, 1988; Natchimuthu et al., 2014), the contribution of ebullition was determined by comparing the flux measured

with the transfer coefficient method against the total flux measured with the floating chambers flux.

#### 2.4. Measurement of Ancillary Variables

Meteorological data (air temperature, air pressure, wind speed, and precipitation) were obtained from the local weather stations, which provided meteorological information at a 30 min interval. During each sampling campaign, surface water temperature, pH, salinity, and dissolved oxygen (DO) concentration at 20 cm water depth were measured *in situ* in each sampling site. Water temperature and pH were measured using a handheld pH/mV/Temperature meter system (IQ150, IQ Scientific Instruments, USA) and the salinity was measured using a salinity meter (Eutech Instruments-Salt6, USA). The dissolved oxygen concentration was determined *in situ* with a multiparameter probe (550A YSI, USA) at 20 cm depth.

During each sampling campaign, surface water samples (~ 20 cm depth) were collected from the above mentioned positions from different zones by using organic glass hydrophores, and then transferred into 150 mL polyethylene bottles. Approximately 0.2 mL of saturated HgCl<sub>2</sub> solution was injected into each bottle to inhibit microbial activity (Zhang et al., 2013; Yang et al., 2017b). The water samples were subsequently transported to the laboratory within 4–6 h, stored in a 4 °C cooler, and analyzed within one week.

Approximately 100 mL of the water sample was filtered through a 0.45 µm filter (Biotrans™ nylon membranes) and subsequently analyzed for the concentrations of N-NO<sub>3</sub><sup>-</sup> and total organic carbon (TOC). N-NO<sub>3</sub><sup>-</sup> and TOC concentrations in the surface water samples were analyzed using flow injection analysis (Skalar Analytical SAN<sup>++</sup>, Netherlands) and a total organic carbon analyzer (Schimadzu TOC-V<sub>CPH/CPN</sub>, Kyoto, Japan), respectively. The detection limits for N-NO<sub>3</sub><sup>-</sup> and TOC were 6 µg L<sup>-1</sup> and 4 µg L<sup>-1</sup>, respectively. The relative standard deviations of N-NO<sub>3</sub><sup>-</sup> and TOC analyses were ≤3.0% and ≤1.0%, respectively.

#### 2.5. Data Analysis

The calculations of basic statistical parameters (e.g. mean, standard error (SE), and others) were carried out using SPSS 17.0 (SPSS, Inc., USA). Data transformations were performed using both the Box-Cox procedure (including CH<sub>4</sub> fluxes | $\lambda$  = -0.12, CH<sub>4</sub> concentrations | $\lambda$  = -0.13, wind speed | $\lambda$  = 0.23, salinity | $\lambda$  = -0.22 and NO<sub>3</sub><sup>-</sup>-N | $\lambda$  = -0.19, and  $\lambda$  herein is the Box-Cox exponent) and log transformation (TOC) to ensure *a priori* that the assumptions for the analyses of variance and the linear model analysis were not violated. Significance tests were calculated based on the transformed data, while untransformed data are used to plot the figures. Two-way analysis of variance (ANOVA) was conducted to analyze the effects of sampling zones (nearshore zone, feeding zone, and aeration zone), culturing time, and their interactions on the CH<sub>4</sub> diffusion fluxes (or CH<sub>4</sub> concentration) in shrimp ponds with ponds specified as the random term. Linear mixed effects models accounting the pond random effect were also fitted to explore the relationships between environmental variables and the CH<sub>4</sub> diffusion fluxes (or CH<sub>4</sub> concentration) using the nlme package of R (Bates et al., 2014; Holgerson, 2015). The stepAIC() function in the R package “MASS” was used for the model selection (Ripley et al., 2016). The model with the

lowest AIC value was chosen, and the relationship between the dependent variables and chosen predictors was further tested by Type II Wald's test implemented in the R package "car" (Fox et al., 2018). To test whether there is a significant random effect, this study used the rand function in the R package "lmerTest" (Kuznetsova et al., 2017) to perform a likelihood ratio test. The Chi square statistics and the corresponding p-values of this test were implemented in the 2-way ANOVA table, and this kind of statistics thus indicate whether the variation in the CH<sub>4</sub> diffusion fluxes (or CH<sub>4</sub> concentration) were dependent on the random pond selection. Other analyses and graphics were conducted with SPSS 17.0 (SPSS, Inc., USA) and OriginPro 7.5 (OriginLab Corporation, USA), respectively. The results were considered significant at the 0.05 significance level and summarized as "mean ± standard error". The concentration and diffusion fluxes of CH<sub>4</sub> data from the three shrimp ponds were interpolated for mapping by using Inverse Distance Weighted method (IDW) in ArcGIS 10.2 (ESRI Inc., Redlands, CA, USA).

### 3. Results

#### 3.1. Meteorological Parameters and Surface Water Quality

The variations in meteorological parameters from the shrimp ponds during the aquaculture period are shown in Figure 2. Atmospheric pressure in the estuarine ponds showed an increasing trend with time (Figure 2a), and the differences were more than 35 hPa ( $p < 0.05$ , ranged from 985 to 1020 hPa). Wind speed (Figure 2a) and air temperature (Figure 2c) from the estuarine ponds varied greatly between months, with considerably higher values from August to October. Meteorological parameters showed insignificantly spatial changes inside and between ponds ( $p > 0.05$ ).

The temporal variations in water quality parameters from the shrimp ponds during the aquaculture period are shown in Figure 3. Water temperature displayed obvious temporal changes, and the mean values changed from 18.11°C (in November) to 34.35°C (in August) (Figure 3a). The other five water quality parameters, namely pH, DO, salinity, N-NO<sub>3</sub><sup>-</sup>, and TOC, also showed prominently temporal changes (Figure 3b-f). Water pH and DO in the shrimp ponds over the study period ranged from 9.11 to 10.01, and from 12.17 to 18.84 mg L<sup>-1</sup>, respectively, with lower pH in July ( $p < 0.05$ ; Figure 3b), and lower DO in September and October ( $p < 0.05$ ; Figure 3c). The mean salinity and N-NO<sub>3</sub><sup>-</sup> concentrations were lower in July and August compared with other months ( $p < 0.05$ ; Figure 3d and 3e). The TOC concentrations of the shrimp ponds was generally between 11.40 and 41.59 mg L<sup>-1</sup> with lower TOC in July and higher value in October ( $p < 0.05$ ; Figure 3f).

The spatial variations in water quality parameters within- and between-ponds during the aquaculture period are shown in Figure S1. Most of the measured water quality variables, namely temperature, pH, salinity, N-NO<sub>3</sub><sup>-</sup> and TOC, did not differ significantly between the sampling sites within-ponds ( $p > 0.05$ ; Figure S1). The differences of mean values of the water quality parameters between three ponds were insignificantly ( $p > 0.05$ ; Figure S1). However, significant differences in DO concentrations were observed between the sampling sites within ponds ( $p < 0.05$ ; Figure S1E), and the average DO concentrations in the Zone F were generally higher

than those in the Zones N and A.

## **3.2. Spatial Variation in CH<sub>4</sub> Concentration and Diffusion Flux**

### **3.2.1. Within-Pond Variation**

Surface water CH<sub>4</sub> concentration from the estuarine shrimp ponds changed considerably between different zones within ponds (Figure 4 and Figure S2). Across all sampling ponds, mean CH<sub>4</sub> concentrations ranged from  $2.19 \pm 0.28$  to  $18.69 \pm 4.17$   $\mu\text{M}$ ,  $4.28 \pm 0.67$  to  $88.82 \pm 17.69$   $\mu\text{M}$ , and  $1.64 \pm 0.15$  to  $9.12 \pm 2.96$   $\mu\text{M}$ , in the Zones N, F and A, respectively, with average values of  $7.84 \pm 1.11$ ,  $33.09 \pm 6.07$  and  $4.01 \pm 0.67$   $\mu\text{M}$ . The CH<sub>4</sub> diffusion flux also showed very large spatial variations across the different zones within ponds (Figure 5 and Figure S2A), ranging from  $0.09 \pm 0.01$  to  $0.86 \pm 0.20$   $\text{mmol m}^{-2} \text{h}^{-1}$ ,  $0.17 \pm 0.02$  to  $4.04 \pm 1.19$   $\text{mmol m}^{-2} \text{h}^{-1}$ , and  $0.06 \pm 0.01$  to  $0.44 \pm 0.14$   $\text{mmol m}^{-2} \text{h}^{-1}$  in the Zones N, F and A, respectively. Over the study period, the Zone F was hot spot of CH<sub>4</sub> emission ( $1.69 \pm 0.33$   $\text{mmol m}^{-2} \text{h}^{-1}$ ), followed by the Zone N ( $0.34 \pm 0.05$   $\text{mmol m}^{-2} \text{h}^{-1}$ ) and Zone A ( $0.19 \pm 0.03$   $\text{mmol m}^{-2} \text{h}^{-1}$ ) (Figure S2A). There were significant differences in pond water CH<sub>4</sub> concentration and fluxes between different zones within ponds ( $p < 0.01$ ; Figure S2A and Table 1).

### **3.2.2. Between-Pond Variation**

Across all sampling months and sites, the mean CH<sub>4</sub> concentrations were  $18.81 \pm 4.79$   $\mu\text{M}$ ,  $11.65 \pm 3.67$   $\mu\text{M}$ , and  $14.48 \pm 3.33$   $\mu\text{M}$  in Ponds I, II and III, respectively (Figure 4). The overall median and mean from all ponds were 4.57 and 14.98  $\mu\text{M}$ . CH<sub>4</sub> concentrations were supersaturated across all ponds during the aquaculture period, indicating that aquaculture ponds are CH<sub>4</sub> emission source (Figure 5). The mean CH<sub>4</sub> emission fluxes were  $0.95 \pm 0.25$   $\text{mmol m}^{-2} \text{h}^{-1}$ ,  $0.58 \pm 0.21$   $\text{mmol m}^{-2} \text{h}^{-1}$ , and  $0.70 \pm 0.17$   $\text{mmol m}^{-2} \text{h}^{-1}$  in Ponds I, II and III, respectively (Figure 5). The overall median and mean of CH<sub>4</sub> fluxes from all three ponds were 0.19 and 0.74  $\text{mmol m}^{-2} \text{h}^{-1}$ , respectively. The CH<sub>4</sub> concentrations and flux in Pond I were largest, followed by Pond III and Pond II (Figures 4 and 5), and there was significant difference in CH<sub>4</sub> concentrations and flux between ponds ( $p < 0.05$ ; Table 1).

## **3.3. Temporal Variation in CH<sub>4</sub> Concentration and Diffusion Flux**

CH<sub>4</sub> concentration and diffusion flux in three shrimp ponds showed similar temporal patterns, with the highest CH<sub>4</sub> concentration and flux generally in August and September, and the lowest flux always in June and November (Figures 5 and 6). When averaging the monthly concentrations (or fluxes) over three ponds, a strong temporal pattern in CH<sub>4</sub> concentrations (or fluxes) emerged, with the minimum in June ( $2.71 \pm 0.33$   $\mu\text{M}$  and  $0.11 \pm 0.01$   $\text{mmol m}^{-2} \text{h}^{-1}$ ), the maximum in September ( $38.88 \pm 9.13$   $\mu\text{M}$  and  $1.76 \pm 0.41$   $\text{mmol m}^{-2} \text{h}^{-1}$ ), and generally low values in November ( $4.89 \pm 0.64$   $\mu\text{M}$  and  $0.17 \pm 0.02$   $\text{mmol m}^{-2} \text{h}^{-1}$ ). According to the AIC-based model selection, monthly CH<sub>4</sub> concentration / flux (temporal variations) in the estuarine ponds were best predicted by dissolved oxygen (DO), atmospheric pressure and salinity / pH (Table 2).

## **4. Discussions**

### **4.1. Role of Dissolved Oxygen and Organic Matter**

Large spatial variation in CH<sub>4</sub> concentration and flux at small spatial scales (e.g., within system, and between systems) has been reported in rivers (Crawford et al., 2017; Zhao et al., 2013), reservoirs (Musenze et al., 2014; Zhao et al., 2013), and lakes (Borges et al., 2011; Chuang et al., 2017; Natchimuthu et al., 2016; Schrier-Uijl et al., 2011; Xiao et al., 2017; Xing et al., 2005; Yang et al., 2008). Many of these studies have attributed the spatial variation of CH<sub>4</sub> concentration and flux to direct or indirect effects of primary productivity, nutrient status (e.g., organic carbon), meteorology, and morphometry (e.g., area and depth) (e.g., Chuang et al., 2017; Holgerson et al., 2015; Natchimuthu et al., 2016; Schrier-Uijl et al., 2011; Xiao et al., 2017; Xing et al., 2006). To the best of our knowledge, such information is limited for aquaculture ponds. In the current research, the small spatial scales variations in CH<sub>4</sub> concentration and flux across the shrimp ponds were analyzed. An interesting finding of this study was CH<sub>4</sub> concentration (or fluxes) differed significantly both within pond and among ponds (Table 1).

The average CH<sub>4</sub> concentration and emission flux in Pond-I was significantly higher than those in Pond-II and Pond-III (Figures 4 and 5;  $p < 0.01$ ). The spatial variability of CH<sub>4</sub> dynamics might be related to the physical and chemical parameters of sediment / water differed in their magnitude among the three ponds, which influence sediment CH<sub>4</sub> production. Among the several environmental variables of the study (Figure S1), only water N-NO<sub>3</sub><sup>-</sup> concentration differed significantly among ponds ( $p < 0.01$ ), and the average concentration followed the orders: Pond-II ( $99.7 \pm 15.7 \mu\text{g L}^{-1}$ ) > Pond-III ( $50.3 \pm 5.1 \mu\text{g L}^{-1}$ ) > Pond-I ( $22.9 \pm 3.1 \mu\text{g L}^{-1}$ ). The spatial patterns of N-NO<sub>3</sub><sup>-</sup> concentration and CH<sub>4</sub> dynamics in the MRE ponds were largely similar. Previous research has shown that some microorganisms preferentially use N-NO<sub>3</sub><sup>-</sup> as an alternative electron acceptor to oxidize organic substrates (such as acetate) in anaerobic environments (Hu et al., 2017; Nykänen et al., 2002), thereby outcompeting methanogens and inhibiting methanogenesis. Therefore, it is considered that high CH<sub>4</sub> emission flux occurred in Pond-I and low flux occurred in Pond-II, to some extent, were dependent on the difference in N-NO<sub>3</sub><sup>-</sup> concentration between ponds.

Net CH<sub>4</sub> release rate in aquatic ecosystems is determined by the production of methanogens, consumption by methanotrophs, and transport processes, which are essentially affected by a series of biotic and abiotic parameters. The role of DO in methane dynamic has been evaluated in various aquatic ecosystems (e.g., Liu et al., 2015; Schrier-Uijl et al., 2011; Xiao et al., 2017; Yang et al., 2015a). High water DO concentration would promote CH<sub>4</sub> oxidation at the sediment-water interface or during the passway in transportation but inhibit methanogens (Liu et al., 2015; Schrier-Uijl et al., 2011), ultimately resulting in a lower water CH<sub>4</sub> concentration and the subsequent emission (Xiao et al., 2017). This study found the Zone F with the smallest surface water DO (Figure S1E) and largest CH<sub>4</sub> concentration (Figure S2A) and diffusion flux (Figure S2B). Also, CH<sub>4</sub> concentration and flux significantly and negatively correlated with DO concentrations ( $p < 0.05$ ; Figures 6 and 7). These results suggested that the DO variations could be one of possible reasons for the difference in CH<sub>4</sub> concentration and flux among the three zones within ponds in our study site.

In addition to DO, sediment total carbon (TC) content (P. Yang, unpublished data) and

water TOC concentration differ markedly between the three zones within ponds. Sediment TC and water TOC (Figure S1G) in the Zone F were largest, followed by the Zones N and A, which was similar to the spatial distribution of water CH<sub>4</sub> concentration and release flux (Figure S2). This indicates that organic matters (e.g., bait) was also a variable causing spatial variations in CH<sub>4</sub> flux inside the pond. It is well known that CH<sub>4</sub> in aquatic ecosystem is mainly generated from sediments containing organic matters (e.g., Bastviken et al., 2008; Grinham et al., 2018; Xiao et al., 2017). Large organic matter loading in sediment not only fuels CH<sub>4</sub> production, but also increases oxygen consumption, which suppresses CH<sub>4</sub> oxidation (Huttunen et al., 2003; Xiao et al., 2017). Consequently, large amounts of CH<sub>4</sub> was produced in the feeding zone and emitted into water and atmosphere. These finding highlights pond aeration (DO) and organic matter supply play an important role in the large spatial variation in CH<sub>4</sub> concentration and flux within pond.

#### **4.2. Factors Influencing the Temporal Variations of CH<sub>4</sub> Flux**

At the month scale, the mean CH<sub>4</sub> concentration and diffusion flux in the three ponds showed considerable variation (Figures 4 and 5). Overall, higher CH<sub>4</sub> concentration and flux occurred in August and September and lower value appeared in June and November. Markedly temporal variations in CH<sub>4</sub> concentration / flux have been reported in lakes (Natchimuthu et al., 2016; Xiao et al., 2017), rivers (Borges et al., 2018; Zhao, et al., 2013), shallow ponds (Holgerson, 2015; Yang et al., 2018a), coastal and continental shelf zones (e.g., Borges et al., 2018; Cunada et al., 2018; Gülzow et al., 2014; Jakobs et al., 2014; Sierra et al., 2017). Most of these studies have related the seasonal patterns of CH<sub>4</sub> with variation in temperature (e.g., Borges, et al., 2017; Natchimuthu et al., 2016; Sierra et al., 2017; Xiao et al., 2017; Yang et al., 2018a; Zhao, et al., 2013), particularly the increase in sediment CH<sub>4</sub> production rates in response to the increasing temperature (Vizza et al., 2017; Yang et al., 2018a; Yvon-Durocher et al., 2014). In addition, some studies found that the seasonal variation of CH<sub>4</sub> could be governed by the changes in DO concentrations in aquatic systems (Holgerson, 2015; Hu et al., 2018; Zhao, et al., 2013). Generally, when DO concentration is low in water, the methanogenic (anaerobic bacteria) activity increases and the CH<sub>4</sub> oxidation capacity declines, which leads to the increase in sediment CH<sub>4</sub> production and subsequent emission (Hu et al., 2018; Ivanov et al., 2002). According to the AIC-based model selection, CH<sub>4</sub> emission fluxes were best predicted by a negative relationship with DO (Table 2), indicating that DO level was also play a major role in influencing the temporal variation in CH<sub>4</sub> emissions from the aquaculture ponds in subtropical estuaries.

Salinity is an important environmental factor governing CH<sub>4</sub> dynamics in coastal areas (Tong et al., 2010; Vizza et al., 2017). On one hand, salinity allows the occurrence of sulfate-reduction that leads to enhanced anaerobic oxidation of CH<sub>4</sub> in sediments, and strong competition of sulfate-reducers with methanogens (Vizza et al., 2017). On the other hand, high salinity induces ion (e.g., Cl<sup>-</sup> and Fe<sup>3+</sup>) stress (Chambers et al., 2013; Neubauer et al., 2013) or harm to methanogens (Sun et al., 2013), with the consequence of reducing sediment CH<sub>4</sub> production. Many studies found CH<sub>4</sub> emission fluxes from coastal wetlands and aquatic ecosystems decreases

with the increase in salinity (e.g., Poffenbarger et al., 2011; Vizza et al., 2017; Welti et al., 2017; Wilson et al., 2015; Yang et al., 2018a). Similarly, the significantly lower water salinity between August and September in this study (Figure 3d) could significantly increase sediment CH<sub>4</sub> production owing to the enhanced methanogenic activities. Thus, the higher concentration and flux of CH<sub>4</sub> in the August and September was likely due to the higher CH<sub>4</sub> production rates supported by lower water salinity. Although CH<sub>4</sub> production data are unavailable in the present study, the CH<sub>4</sub> concentration in the ponds showed a significantly negative relationship with water salinity ( $p < 0.05$ ; Table 2), which supports the above hypothesis. Further studies merit to explore the exact impacts of salinity on CH<sub>4</sub> production and emission.

Previous studies show that low pressures may facilitate the transport of CH<sub>4</sub> from sediments to the atmosphere and reduce the amount of time available for methane oxidation (Chen et al., 2014; Natchimuthu et al., 2014, 2016; Zhu et al., 2016). This study observed high CH<sub>4</sub> concentration and flux in the August and September and low values in the June and November, which were opposite to the trend of atmospheric pressure ( $p < 0.05$ ; Table 2). The results showed that the seasonal variation of ponds CH<sub>4</sub> dynamics in the aquaculture ponds also could be governed by the changes in atmospheric pressure.

In addition, this study also found a significantly positive relationship between monthly CH<sub>4</sub> flux and pH ( $p < 0.01$ ; Table 2). Methanogens are pH sensitive and grow best around pH 6–8 in wetland and aquatic systems (Chang and Yang, 2003; Hu et al., 2017; Yang et al., 2017b). Hence CH<sub>4</sub> flux is expected to decrease as pH values move away from the optimal range of 6–8 (e.g., Hu et al., 2017; Le Mer and Roger, 2001; Schrier-Uijl et al., 2011). The positive relationship observed between CH<sub>4</sub> flux and pH in this study could be related, at least in part, to the influence of primary production. A higher primary production will enhance the uptake of CO<sub>2</sub> in the water column, which in turn increase water pH and alkalinity (Gruca-Rokosz et al., 2017; Portielje and Lijklema, 1995). At the same time, a higher primary production can increase the supply of organic matter to pond sediments, thereby reducing soil redox potential and stimulating methanogenic activities. Further studies should be done using controlled experiments to examine whether pH exerts a direct influence on CH<sub>4</sub> emissions.

#### **4.3. Diffusion isn't a Major Pathway of CH<sub>4</sub> Emission in Mariculture Pond**

Anoxic sediment is “hot spot” of methane production in aquatic ecosystems. Methane can be exported from the sediment through molecule diffusion, ebullition (bubbles), or combination of them (Bastviken et al., 2004; Hu et al., 2016). Ebullition is often considered as the main CH<sub>4</sub> emission pathway in reservoirs, rivers and lakes (e.g., Bastviken et al., 2004; Chuang et al., 2017; Deshmukh et al., 2014; Natchimuthu et al., 2016; Rodriguez and Casper, 2018; Xiao et al., 2017). However, such information from aquaculture ponds is still very limited (Yang et al., 2017a). In the current research, the contribution of ebullition was estimated by comparing the diffusion flux measured with the transfer coefficient method against the total flux measured with the floating chambers (Bastviken et al., 2004; Chuang et al., 2017; Keller and Stallard, 1994; Miller and Oremland, 1988; Natchimuthu et al., 2014). The average CH<sub>4</sub>

diffusion flux and total flux ranged from 0.11 to 1.76 mmol m<sup>-2</sup> h<sup>-1</sup> and 0.18 to 8.52 mmol m<sup>-2</sup> h<sup>-1</sup> (Figure S3), respectively, with mean values of 0.74 ± 0.30 and 3.86 ± 1.38 mmol m<sup>-2</sup> h<sup>-1</sup>, respectively. Consequently, the average CH<sub>4</sub> ebullition flux ranged from 0.01 to 6.98 mmol m<sup>-2</sup> h<sup>-1</sup>, with mean values of 3.12 ± 1.21 mmol m<sup>-2</sup> h<sup>-1</sup> (Figure S3). Ebullition emission comprises over 70% (ranged 5.0 to 96.3%) of the total CH<sub>4</sub> flux. In spite of limited number of floating chambers, our results clearly show that CH<sub>4</sub> emission was dominated by ebullition. In the meantime, our results highlight that diffusion isn't the main CH<sub>4</sub> emission pathway in aquaculture ponds. Given the episodic nature of ebullition (Xiao et al., 2017), obviously more fine-scale temporal and spatial measurements data are needed to increase the accuracy in the flux estimate.

#### **4.4. Implications of CH<sub>4</sub> Emission Flux from Aquaculture Ponds**

##### **4.4.1. Implications of CH<sub>4</sub> Flux Spatiotemporal Variations**

Our results highlight that subtropical aquaculture ponds are large atmospheric CH<sub>4</sub> sources with strong spatial variability. The large spatial variation of CH<sub>4</sub> flux within ponds (Figure S2) implies a large uncertainty of whole-pond CH<sub>4</sub> fluxes budgets estimated by earlier studies that based on single or limited number of site measurements (e.g., Hu et al., 2016; Ma et al., 2018; Yang et al., 2017a; Yang et al., 2018a). For a more accurate estimate of whole pond CH<sub>4</sub> emissions, it is of paramount importance to take into account of measurements from a number of strategically located sites that would adequately capture a representative areal extent of the emitting surface. The markedly spatial variation in CH<sub>4</sub> fluxes means that extrapolation of a few ponds' measurements during regional CH<sub>4</sub> budgeting should be done cautiously. Similarly, the significant temporal variation of pond CH<sub>4</sub> fluxes (Figure 5) implies the large uncertainty during extrapolating a single month CH<sub>4</sub> emission measurement to annual emissions. Therefore, it is very important to measure from as many sites as practicable over a number of months in order to reduce the uncertainty of CH<sub>4</sub> flux estimations and improve our understanding of CH<sub>4</sub> dynamics in aquaculture ponds.

##### **4.4.2. Implications of Large CH<sub>4</sub> Emission Flux**

An earlier study estimated that GHGs (CO<sub>2</sub> and CH<sub>4</sub>) efflux from mariculture ponds across the subtropical estuaries of China would be equivalent to ~15% of the net carbon emissions from the terrestrial natural ecosystems in China (Yang et al., 2018a). It is worth noting that the CH<sub>4</sub> emissions fluxes in subtropical estuarine aquaculture ponds were substantially higher than those from the freshwater aquaculture systems (e.g., Da Silva et al., 2018; Hu et al., 2014; Hu et al., 2016; Liu et al., 2015; Wu et al., 2018) and were one to three orders of magnitude larger than those observed in most reservoirs and lakes (e.g., Gerardo-Nieto et al., 2017; Huttunen et al., 2003; Musenze et al., 2014; Natchimuthu et al., 2016; Wen et al., 2016; Xiao et al., 2017; Zhao et al., 2013; Zhu et al., 2010). CH<sub>4</sub> diffusion fluxes in our ponds were also substantially higher than those in coastal aquatic ecosystems (Sierra et al., 2017), and was approximately 8 times higher than the average of 0.09 mmol m<sup>-2</sup> h<sup>-1</sup> found in China's natural wetlands (Wei and Wang, 2017). Moreover, the magnitude of CH<sub>4</sub> emissions observed in our ponds were much larger than those from the estuarine brackish

*Cyperus malaccensis* marsh (ranged from 0.04 to 0.32 mmol m<sup>-2</sup> h<sup>-1</sup>) (Yang et al., 2019). These results suggest that subtropical estuarine aquaculture ponds could be important sources of atmospheric CH<sub>4</sub>, which could play an important yet overlooked role in regional and global CH<sub>4</sub> budgets.

It is a big challenge to balance the economic development and environmental protection (Yang, 2014), for example seafood production and CH<sub>4</sub> mitigation from subtropical estuarine aquaculture ponds. This study found that the Zone F was hot spot of CH<sub>4</sub> emission, followed by the Zone N and A (Figure 5 and Figure S2), which accounting for approximately 60%, 26% and 14% of total pond CH<sub>4</sub> emission fluxes, respectively. Aquaculture ponds are generally maintained through daily feed supply to produce aquatic animals (Chen et al., 2015, 2016). However, only a small portion of the feed input is actually converted into shrimp biomass, with the feed utilization efficiency of ~4.0%–27.4% (Chen et al., 2015; Molnar et al., 2013). Most of the feed input remains in aquaculture systems. Thus large CH<sub>4</sub> emission fluxes occurred the feeding zone, to a large extent, were dependent on the plentiful supply of organic matter from residual feed and faeces, which are more favorable for the majority of CH<sub>4</sub> production. These findings indicate that improving feed utilization efficiency, reducing organic matter (e.g., residual feed and faeces) accumulation on the bottom of ponds feeding zone, and increasing the area of aeration activities might be important strategies to mitigate CH<sub>4</sub> emissions from aquaculture ponds.

#### **4.5. Limitation and Future Research**

Similar as many studies, there are some limitations in the current study. CH<sub>4</sub> measurement and estimation were conducted in one estuary during the aquaculture period (from June to November) in the present study. Significantly spatiotemporal variations in CH<sub>4</sub> fluxes at various sites in different shrimp ponds have been found in our study. Obviously, future research should increase the frequency of *in situ* sampling and include more innovative techniques to measure CH<sub>4</sub> flux in aquaculture ponds at multiple estuaries. Moreover, our study did not thoroughly quantify event-driven CH<sub>4</sub> exchange, such as the effect of weather conditions, particularly the extreme weather (e.g., typhoon), on water-atmosphere CH<sub>4</sub> fluxes. Many previous studies have found a large amount of ebullition coinciding with a low atmosphere pressure (Casper et al., 2000; Chen et al., 2014; Mattson & Likens, 1990; Natchimuthu et al., 2015, 2016). Thereby many low pressure induced CH<sub>4</sub> flux events were likely missed, in turn generating underestimated CH<sub>4</sub> fluxes (Natchimuthu et al., 2016). Event-driven CH<sub>4</sub> fluxes during the sampling period should be further investigated. Furthermore, CH<sub>4</sub> fluxes in the aquatic systems varied greatly in diurnal cycle (e.g., Erkkilä et al., 2018; Hirota et al., 2007; Natchimuthu et al., 2014; Xing et al., 2004). Most of the research found that high CH<sub>4</sub> flux generally occurred during the daytime and low flux occurred during the nighttime (e.g., Bastviken et al., 2004; Hirota et al., 2007; Natchimuthu et al., 2014; Xing et al., 2004). In spite of no direct measurement of day-night pattern of CH<sub>4</sub> fluxes in the current study, a similar diurnal pattern can happen in aquaculture ponds. Therefore, increase in sampling frequency in the further studies can improve the estimate accuracy of CH<sub>4</sub> fluxes at diurnal temporal scales before upscaling them to calculate seasonal and annual flux.

Significant amount of CH<sub>4</sub> ebullition fluxes in shrimp ponds have been found in our study, which are consistent with those of previous studies in shallow and nutrient-rich ponds (e.g., [Holgerson, 2015](#); [Natchimuthu et al., 2014](#)). However, the accuracy of our estimates was eroded due to the CH<sub>4</sub> ebullition fluxes was estimated by comparing the diffusion flux measured with the transfer coefficient method against the total flux measured with the floating chambers. In the future work, therefore, there is an urgent need for utilizing advancing technologies to directly measure the CH<sub>4</sub> ebullition in aquaculture ponds.

## 5. Conclusions

CH<sub>4</sub> concentrations were supersaturated across all ponds and all sampling dates, indicating that aquaculture shrimp ponds were important CH<sub>4</sub> emitters to the atmosphere. CH<sub>4</sub> emissions from the estuarine ponds varied greatly between months, reaching a peak in August and September, which was similar to the trend of temperature and water DO concentrations. Duplicate CH<sub>4</sub> measurements at various sites within ponds yielded new insights into the spatial variations of CH<sub>4</sub> concentration and emission flux. The patterns clearly show that the common single-point is not representative for estimating whole-pond CH<sub>4</sub> emissions. The integrated assessment of both spatial (at various sites within pond) and temporal variations in this study showed that it is important to measure from as many sites as practicable over a number of months to improve the accuracy of whole-pond CH<sub>4</sub> flux estimates. Mariculture shrimp ponds in the subtropical estuaries are large sources of atmospheric CH<sub>4</sub>. The high spatial CH<sub>4</sub> flux variation within ponds implies better aeration and higher feed utilization efficiency would help to mitigate CH<sub>4</sub> emissions from mariculture ponds.

## Acknowledgments

This research was financially supported by the National Science Foundation of China (No. 41671088), the Study-Abroad Grant Project for Graduates of the School of Geographical Sciences, the Graduated Student Science and Technology Innovation Project of the School of Geographical Science, Fujian Normal University (GY201601), Fujian Normal University 2018 provincial college Training Program Project Subsidy (No. 201810394070), Open fund by Jiangsu Key Laboratory of Atmospheric Environment Monitoring and Pollution Control (KHK1806), A Project Funded by the Priority Academic Program Development of Jiangsu Higher Education Institutions (PAPD) and Minjiang Scholar Programme. Authors would like to thank Qianqian Guoa, Ling Lia, and Guanghui Zhao of the School of Geographical Sciences, Fujian Normal University, for their field assistance. The data used in this study are available in the Article File, Data Set File and Supporting Material File.

## References

- Abril, G., Commarieu, M. V., & Guérin F. (2007). Enhanced methane oxidation in an estuarine turbidity maximum. *Limnology and Oceanography*, 52, 470-475. <https://doi.org/10.4319/lo.2007.52.1.0470>
- Bastviken, D., Cole, J., Pace, M., & Tranvik, L. (2004). Methane emissions from lakes: Dependence of lake characteristics, two regional assessments, and a global estimate. *Global Biogeochemical Cycles*, 18, GB4009. <https://doi.org/10.1029/2004GB002238>

- Bastviken, D., Cole, J. J., Pace, M. L., & Van de Bogert, M. C. (2008). Fates of methane from different lake habitats: connecting whole-lake budgets and CH<sub>4</sub> emissions. *Journal of Geophysical Research: Biogeosciences*, *113*, G02024. <https://doi.org/10.1029/2007JG000608>
- Bastviken, D., Tranvik, L. J., Downing, J. A., Crill, P. M., & Enrich-Prast, A. (2011). Freshwater methane emissions offset the continental carbon sink. *Science*, *331*, 50. <https://doi.org/10.1126/science.1196808>
- Blees, J., Niemann, H., Erne, M., Zopfi, J., Schubert, C. J., & Lehmann, M. F. (2015). Spatial variations in surface water methane super-saturation and emission in Lake Lugano, southern Switzerland. *Aquatic Sciences*, *77*, 535-545. <https://doi.org/10.1007/s00027-015-0401-z>
- Borges, A. V., Speeckaert, G., Champenois, W., Scranton, M. I., & Gypens, N. (2018). Productivity and temperature as drivers of seasonal and spatial variations of dissolved methane in the Southern Bight of the North Sea. *Ecosystems*, *21*(4), 583-599. <https://doi.org/10.1007/s10021-017-0171-7>
- Borges, A. V., Darchambeau, F., Teodoru, C. R., Marwick, T. R., Tamooch, F., Geeraert, N., Omengo, F. O., Guérin, F., Lambert, T., Morana, C., Okuku, E., & Bouillon, S. (2015). Globally significant greenhouse gas emissions from African inland waters. *Nature Geoscience*, *8*, 637-642. [doi:10.1038/NGEO2486](https://doi.org/10.1038/NGEO2486)
- Borges, A.V., Abril, G., Delille, B., Descy, J.-P., Darchambeau, F. (2011). Diffusive methane emissions to the atmosphere from Lake Kivu (Eastern Africa). *Journal of Geophysical Research-Biogeosciences*, *116*, G03032. [doi:10.1029/2011JG001673](https://doi.org/10.1029/2011JG001673)
- Casper, P., Maberly, S. C., Hall, G. H., & Finlay, B. J. (2000). Fluxes of methane and carbon dioxide from a small productive lake to the atmosphere. *Biogeochemistry*, *49*(1), 1-19.
- Chambers, L. G., Osborne, T. Z., & Reddy, K. R. (2013). Effect of salinity-altering pulsing events on soil organic carbon loss along an intertidal wetland gradient: a laboratory experiment. *Biogeochemistry*, *115* (1-3), 363-383.
- Chang, T. C., & Yang, S. S. (2003). Methane emissions from wetlands in Taiwan. *Atmospheric Environment*, *37*, 4551-4558. [https://doi.org/10.1016/S1352-2310\(03\)00588-0](https://doi.org/10.1016/S1352-2310(03)00588-0)
- Chen, Y., Mutelet, F., & Jaubert, J. N. (2014). Solubility of carbon dioxide, nitrous oxide and methane in ionic liquids at pressures close to atmospheric. *Fluid Phase Equilibria*, *372*, 26-33. <https://doi.org/10.1016/j.fluid.2014.03.015>
- Chen, Y., Dong, S. L., Wang, Z. N., Wang, F., Gao, Q. F., Tian, X. L., & Xiong, Y. H. (2015). Variations in CO<sub>2</sub> fluxes from grass carp *Ctenopharyngodon idella* aquaculture polyculture ponds. *Aquaculture Environment Interactions*, *8*, 31-40. <https://doi.org/10.3354/aei00149>
- Chen, Y., Dong, S. L., Wang, F., Gao, Q. F., & Tian, X. L. (2016). Carbon dioxide and methane fluxes from feeding and no-feeding mariculture ponds. *Environmental Pollution*, *212*, 489-497. <https://doi.org/10.1016/j.envpol.2016.02.039>
- Chuang, P. -C., Young, M. B., Dale, A. W., Miller, L. G., Herrera-Silveira, J. A., & Paytan, A. (2017). Methane fluxes from tropical coastal lagoons surrounded by mangroves, Yucatán, Mexico. *Journal of Geophysical Research: Biogeosciences*, *122*(5), 1156-1174. <https://doi.org/10.1002/2017JG003761>
- Cole, J. J., & Caraco, N. F. (1998). Atmospheric exchange of carbon dioxide in a low-wind oligotrophic lake measured by the addition of SF<sub>6</sub>. *Limnology and Oceanography*, *43*(4), 647-656. <https://doi.org/10.4319/lo.1998.43.4.0647>
- Cotovicz Jr., L. C., Knoppers, B. A., Brandini, N., Poirier, D., Costa Santos, S. J., & Abril, G. (2016). Spatio-temporal variability of methane (CH<sub>4</sub>) concentrations and diffusive fluxes from a tropical coastal embayment surrounded by a large urban area (Guanabara Bay, Rio de Janeiro, Brazil). *Limnology and Oceanography*, *61*(S1), <https://doi.org/10.1002/lno.10298>
- Crawford, J. T., Loken, L. C., West, W. E., Crary, B., Spawn, S. A., Gubbins, N., Jones, S. E., Striegl, R. G., & Stanley, E. H. (2017). Spatial heterogeneity of within-stream methane concentrations. *Journal of Geophysical Research: Biogeosciences*, *122*, 1036-1048. <https://doi.org/10.1002/2016JG003698>

- Crusius, J., & Wanninkhof, R. (2003). Gas transfer velocities measured at low wind speed over a lake. *Limnology and Oceanography*, 48(3), 1010-1017. <https://doi.org/10.4319/lo.2003.48.3.1010>
- Cunada, C. L., Lesack, L. F. W., & Tank, S. E. (2018). Seasonal dynamics of dissolved methane in lakes of the Mackenzie Delta and the role of carbon substrate quality. *Journal of Geophysical Research: Biogeosciences*, 123(2), 591-609. <https://doi.org/10.1002/2017JG004047>
- Da Silva, M. G., Packer, A. P., Sampaio, F. G., Marani, L., Mariano, E. V. C., Pazianotto, R. A. A., Ferreira, W. J., & Alvalá, P. C. (2018). Impact of intensive fish farming on methane emission in a tropical hydropower reservoir. *Climatic Change*, 150(3-4), 195-210. <https://doi.org/10.1007/s10584-018-2281-4>
- Deshmukh, C., Guérin, F., Labat, D., Pighini, S., Vongkhamsoo, A., Guédant, P., Rode, W., Godon, A., Chanudet, V., Descloux, S., & Serça, D. (2016). Low methane (CH<sub>4</sub>) emissions downstream of a monomictic subtropical hydroelectric reservoir (Nam Theun 2, Lao PDR). *Biogeosciences*, 13(6), 1919-1932. <https://doi.org/10.5194/bg-13-1919-2016>
- Diem, T., Koch, S., Schwarzenbach, S., Wehrli, B., & Schubert, C. J. (2012). Greenhouse gas emissions (CO<sub>2</sub>, CH<sub>4</sub>, and N<sub>2</sub>O) from several perialpine and alpine hydropower reservoirs by diffusion and loss in turbines. *Aquatic Sciences*, 74, 619-635. <https://doi.org/10.1007/s00027-012-0256-5>
- Erkkilä, K. M., Ojala, A., Bastviken, D., Biermann, T., Heiskanen, J. J., Lindroth, A., Peltola, O., Rantakari, M., Vesala, T., & Mammarella, I. (2018). Methane and carbon dioxide fluxes over a lake: comparison between eddy covariance, floating chambers and boundary layer method. *Biogeosciences*, 15(2), 429-445. <https://doi.org/10.5194/bg-15-429-2018>
- FAO, 2017. Fishery and aquaculture statistics (global aquaculture production 1950-2014). FishStatJ. <http://www.fao.org/fishery/statistics/software/fishstatj/en>.
- Fariás, L., Sanzana, K., Sanhueza-Guevara, S., & Yevenes, M. A. (2017). Dissolved methane distribution in the Reloncaví Fjord and adjacent marine system during austral winter (41°-43° S). *Estuaries and Coasts*, 40(6), 1592-1606. <https://doi.org/10.1007/s12237-017-0241-2>.
- Fox, J., Weisberg, S., Adler, D., Bates, D. et al. (2018). Package 'car'. <https://cran.rproject.org/web/packages/car/index.html>.
- Gerardo-Nieto, O., Astorga-España, M. S., Mansilla, A., & Thalasso, F. (2017). Initial report on methane and carbon dioxide emission dynamics from sub-Antarctic freshwater ecosystems: a seasonal study of a lake and a reservoir. *Science of the Total Environment*, 593, 144-154. <https://doi.org/10.1016/j.scitotenv.2017.02.144>
- Grinham, A., Dunbabin, M., & Albert, S. (2018). Importance of sediment organic matter to methane ebullition in a sub-tropical freshwater reservoir. *Science of the Total Environment*, 621, 1199-1207. <https://doi.org/10.1016/j.scitotenv.2017.10.108>
- Gülzow, W., Gräwe, U., Kedzior, S., Schmale, O., & Rehder, G. (2014). Seasonal variation of methane in the water column of Arkona and Bornholm Basin, western Baltic Sea. *Journal of Marine Systems*, 139, 332-347. <https://doi.org/10.1016/j.jmarsys.2014.07.013>
- Hirota, M., Senga, Y., Seike, Y., Nohara, S., & Kunii, H. (2007). Fluxes of carbon dioxide, methane and nitrous oxide in two contrastive fringing zones of coastal lagoon, Lake Nakaumi, Japan. *Chemosphere* 68(3), 597-603. <https://doi.org/10.1016/j.chemosphere.2007.01.002>
- Hu, M. J., Ren, H. C., Ren, P., Li, J. B., Wilson, B. J., & Tong, C. (2017). Response of gaseous carbon emissions to low-level salinity increase in tidal marsh ecosystem of the Min River estuary, southeastern China. *Journal of Environmental Sciences*, 52, 210-222. <https://doi.org/10.1016/j.jes.2016.05.009>
- Hu, Z., Lee, J. W., Chandran, K., Kim, S., Sharma, K., & Khanal, S. K. (2014). Influence of carbohydrate addition on nitrogen transformations and greenhouse gas emissions of intensive aquaculture system. *Science of the Total Environment*, 470, 193-200. <https://doi.org/10.1016/j.scitotenv.2013.09.050>
- Hu, Z. Q., Wu, S., Ji, C., Zou, J. W., Zhou, Q. S., & Liu, S. W. (2016). A comparison of methane emissions following rice paddies conversion to crab-fish farming wetlands in southeast China. *Environmental Science and Pollution Research*, 23(2), 1505-1515. <https://doi.org/10.1007/s11356-015-5383-9>

- Holgerson, M. A. (2015). Drivers of carbon dioxide and methane supersaturation in small, temporary ponds. *Biogeochemistry*, 124(1-3), 305-318. <https://doi.org/10.1007/s10533-015-0099-y>
- Holgerson, M. A., & Raymond, P. A. (2016). Large contribution to inland water CO<sub>2</sub> and CH<sub>4</sub> emissions from very small ponds. *Nature Geoscience*, 9(3), 222-226. [doi:10.1038/ngeo2654](https://doi.org/10.1038/ngeo2654)
- Huttunen, J. T., Alm, J., Liikanen, A., Juutinen, S., Larmola, T., Hammar, T., Silvola, J., & Martikainen, P. J. (2003). Fluxes of methane, carbon dioxide and nitrous oxide in boreal lakes and potential anthropogenic effects on the aquatic greenhouse gas emissions. *Chemosphere*, 52(3), 609-621. [https://doi.org/10.1016/s0045-6535\(03\)00243-1](https://doi.org/10.1016/s0045-6535(03)00243-1)
- IPCC. 2013. Climate Change 2013: The Physical Science Basis. Contribution of Working Group I to the Fifth Assessment Report of the Intergovernmental Panel on Climate Change. In T. F. Stocker, and others [eds.], Cambridge Univ. Press. [doi:10.1017/CBO9781107415324](https://doi.org/10.1017/CBO9781107415324).
- Jahne, B., Munnich, K. O., Bosinger, R., Dutzi, A., Huber, W., & Libner, P. (1987). On parameters influencing air-water exchange. *Journal of Geophysical Research: Oceans*, 92, 1937-1949. <https://doi.org/10.1029/JC092iC02p01937>
- Jakobs, G., Holtermann, P., Berndmeyer, C., Rehder, G., Blumenberg, M., Jost, G., & Schmale, O. (2014). Seasonal and spatial methane dynamics in the water column of the central Baltic Sea (Gotland Sea). *Continental Shelf Research*, 91, 12-25. <https://doi.org/10.1016/j.csr.2014.07.005>
- Ivanov, M. V., Pimenov, N. V., Rusanov, I. I., & Lein, A. Y. (2002). Microbial processes of the methane cycle at the north-western shelf of the Black Sea. *Estuarine, Coastal and Shelf Science*, 54(3), 589-599. <https://doi.org/10.1006/ecss.2000.0667>
- Keller, M., & Stallard, R. F. (1994). Methane emission by bubbling from Gatun Lake, Panama. *Journal of Geophysical Research: Atmospheres*, 99, 8307-8319. <https://doi.org/10.1029/92JD02170>
- Kuznetsova, A., Brockhoff, P. B., & Christensen, R. H. B. (2017). *lmerTest* package: tests in linear mixed effects models. *Journal of Statistical Software*, 82(13).
- Le Mer, J., & Roger, P. (2001). Production oxidation emission and consumption of methane by soils: a review. *European Journal of Soil Biology*, 37(1), 25-50. [https://doi.org/10.1016/S1164-5563\(01\)01067-6](https://doi.org/10.1016/S1164-5563(01)01067-6)
- Liss, P. S., & Merlivat, L. (1986). Air-Sea gas exchange rates: introduction and synthesis. In *The Role of Air-Sea Exchange in Geochemical Cycling*. In: Buat-Menard P, (eds.). Reidel: Dordrecht, The Netherlands, pp. 113-129.
- Liu, S. W., Hu, Z. Q., Wu, S., Li, S. Q., Li, Z. F., Zou, J. W. (2015). Methane and nitrous oxide emissions reduced following conversion of rice paddies to inland crab-fish aquaculture in southeast China. *Environmental Science & Technology*, 50(2), 633-642. <https://doi.org/10.1021/acs.est.5b04343>
- Ma, Y. C., Sun, L. Y., Liu, C. Y., Yang, X. Y., Zhou, W., Yang, B., Schwenke, G., & Liu, D. L. (2018). A comparison of methane and nitrous oxide emissions from inland mixed-fish and crab aquaculture ponds. *Science of The Total Environment*, 637-638, 517-523. <https://doi.org/10.1016/j.scitotenv.2018.05.040>
- MacIntyre, S., Wanninkhof, R., & Chanton, J. P. (1995). Trace gas exchange across the air-water interface in freshwater and coastal marine environment. In: Matson, P.A., Harriss, R.C., (eds.). *Biogenic Trace Gases: Measuring Emission from Soil and Water*. Cambridge: Blackwell Scientific Publications Ltd, 52-97.
- Mattson, M. D., & Likens, G. E. (1990). Air pressure and methane fluxes. *Nature*, 347(6295), 718-719.
- Miller, L. G., & Oremland, R. S. (1988). Methane efflux from the pelagic regions of four lakes. *Global Biogeochemical Cycles*, 2, 269-277. <https://doi.org/10.1029/GB002i003p00269>
- Molnar, N., Welsh, D. T., Marchand, C., Deborde, J., & Meziane, T. (2013). Impacts of shrimp farm effluent on water quality, benthic metabolism and N-dynamics in a mangrove forest (New Caledonia). *Estuarine, Coastal and Shelf Science*, 117, 12-21. <https://doi.org/10.1016/j.ecss.2012.07.012>
- Musenze, R. S., Grinham, A., Werner, U., Gale, D., Sturm, K., Udy, J., & Yuan, Z. G. (2014). Assessing the spatial and temporal variability of diffusive methane and nitrous oxide

- emissions from subtropical freshwater reservoirs. *Environmental Science & Technology*, 48, 14499-14507. <https://doi.org/10.1021/es505324h>
- Natchimuthu, S., Selvam, B. P., & Bastviken, D. (2014). Influence of weather variables on methane and carbon dioxide flux from a shallow pond. *Biogeochemistry*, 119(1-3), 403-413. <https://doi.org/10.1007/s10533-014-9976-z>
- Natchimuthu, S., Sundgren, I., Gålfalk, M., Klemedtsson, L., Crill, P., Danielsson, Å., & Bastviken, D. (2016). Spatio-temporal variability of lake CH<sub>4</sub> fluxes and its influence on annual whole lake emission estimates. *Limnology and Oceanography*, 61(S1), S13-S26. <https://doi.org/10.1002/lno.10222>
- Natchimuthu, S., Sundgren, I., Gålfalk, M., Klemedtsson, L., & Bastviken, D. (2017). Spatiotemporal variability of lake pCO<sub>2</sub> and CO<sub>2</sub> fluxes in a hemiboreal catchment. *Journal of Geophysical Research: Biogeosciences*, 122, 30-49. <https://doi.org/10.1002/2016JG00344>
- Neubauer, S. C., Franklin, R. B., & Berrier, D. J. (2013). Saltwater intrusion into tidal freshwater marshes alters the biogeochemical processing of organic carbon. *Biogeosciences*, 10, 8171-8183. <https://doi.org/10.5194/bg-10-8171-2013>
- Nykänen, H., Vasander, H., Huttunen, J. T., & Martikainen, P. J. (2002). Effect of experimental nitrogen load on methane and nitrous oxide fluxes on ombrotrophic boreal peatland. *Plant and Soil*, 242, 147-155.
- Poffenbarger, H. J., Needelman, B. A., & Megonigal, J. P. (2011). Salinity influence on methane emissions from tidal marshes. *Wetlands*, 31, 831-842. <https://doi.org/10.1007/s13157-011-0197-0>
- Raymond, P., & Cole, J. (2001). Gas exchange in rivers and estuaries: Choosing a gas transfer velocity. *Estuaries*, 24(2), 312-317. <https://doi.org/10.2307/1352954>
- Ripley, B., Venables, B., Bates, D. M., Hornil, K., Gebhardt, A., & Firth, D. (2016). [Support Functions and Datasets for Venables and Ripley's MASS. R packag.](#)
- Rodriguez, M., & Casper, P. (2018). Greenhouse gas emissions from a semi-arid tropical reservoir in northeastern Brazil. *Regional Environmental Change*, 18, 1901-1912. <https://doi.org/10.1007/s10113-018-1289-7>
- Schrier-Uijl, A. P., Veraart, A. J., Leffelaar, P. A., Berendse, F., & Veenendaal, E. M. (2011). Release of CO<sub>2</sub> and CH<sub>4</sub> from lakes and drainage ditches in temperate wetlands. *Biogeochemistry*, 102, 265-279. <https://doi.org/10.1007/s10533-010-9440-7>
- Sierra, A., Jiménez-López, D., Ortega, T., Ponce, R., Bellanco, M. J., Sánchez-Leal, R., Gómez-Parra, A., & Forj, J. (2017). Spatial and seasonal variability of CH<sub>4</sub> in the eastern Gulf of Cadiz (SW Iberian Peninsula). *Science of the Total Environment*, 590-591, 695-707. <https://doi.org/10.1016/j.scitotenv.2017.03.030>
- Sun, Z. G., Wang, L. L., Tian, H. Q., Jiang, H. H., Mou, X. J., & Sun, W. L. (2013). Fluxes of nitrous oxide and methane in different coastal *Suaeda salsa* marshes of the Yellow River estuary, China. *Chemosphere*, 90(2), 856-865. <https://doi.org/10.1016/j.chemosphere.2012.10.004>
- Tangen, B. A., Finocchiaro, R. G., Gleason, R. A., & Dahl, C. F. (2016). Greenhouse gas fluxes of a shallow lake in south-central North Dakota, USA. *Wetlands*, 36, 779 -787. <https://doi.org/10.1007/s13157-016-0782-3>
- Tong, C., Wang, W. Q., Zeng, C. S., & Marrs, R. (2010). Methane emissions from a tidal marsh in the Min River estuary, southeast China. *Journal of Environmental Science and Health Part A*, 45, 506-516. <https://doi.org/10.1080/10934520903542261>
- Tong, C., Wang, W. Q., Huang, J. F., Gauci, V., Zhang, L. H., & Zeng, C. S. (2012). Invasive alien plants increase CH<sub>4</sub> emissions from a subtropical tidal estuarine wetland. *Biogeochemistry*, 111, 677-693. <https://doi.org/10.1007/s10533-012-9712-5>
- Vizza, C., West, W. E., Jones, S. E., Hart, J. A., & Lamberti, G. A. (2017). Regulators of coastal wetland methane production and responses to simulated global change. *Biogeosciences*, 14, 431-446. <https://doi.org/10.5194/bg-14-431-2017>
- Wanninkhof, R. (1992). Relationship between wind speed and gas exchange over the ocean. *Journal of Geophysical Research: Oceans*, 97(C5), 7373-7382. <https://doi.org/10.1029/92JC00188>
- Wei, D., & Wang, X. D. (2017). Uncertainty and dynamics of natural wetland CH<sub>4</sub> release in

- China: research status and priorities. *Atmospheric Environment*, 154, 95-105.  
<https://doi.org/10.1016/j.atmosenv.2017.01.038>
- Welti, N., Hayes, M., & Lockington, D. (2017). Seasonal nitrous oxide and methane emissions across a subtropical estuarine salinity gradient. *Biogeochemistry*, 132, 55-69.  
<https://doi.org/10.1007/s10533-016-0287-4>
- Wen, Z. D., Song, K. S., Zhao, Y., & Jin, X. L. (2016). Carbon dioxide and methane supersaturation in lakes of semi-humid/semi-arid region, Northeastern China. *Atmospheric Environment*, 138, 65-73. <https://doi.org/10.1016/j.atmosenv.2016.05.009>
- Wilson, B.J., Mortazavi, B., & Kiene, R. P. (2015). Spatial and temporal variability in carbon dioxide and methane exchange at three coastal marshes along a salinity gradient in a northern Gulf of Mexico estuary. *Biogeochemistry*, 123, 329-347.  
<https://doi.org/10.1007/s10533-015-0085-4>
- World Meteorological Organization, 2016. WMO Greenhouse Gas Bulletin No.12 (October 2016).  
[https://library.wmo.int/opac/doc\\_num.php?explnum\\_id=3084](https://library.wmo.int/opac/doc_num.php?explnum_id=3084). pdf.
- Wu, S., Hu, Z. Q., Hu, T., Chen, J., Yu, K., Zou, J. W., & Liu, S. W. (2018). Annual methane and nitrous oxide emissions from rice paddies and inland fish aquaculture wetlands in southeast China. *Atmospheric Environment*, 175, 135-144.  
<https://doi.org/10.1016/j.atmosenv.2017.12.008>
- Xiao, Q. T., Zhang, M., Hu, Z. H., Gao, Y. Q., Hu, C., Liu, C., Liu, S. D., Zhang, Z., Zhao, J. Y., Xiao, W., & Lee, X. (2017). Spatial variations of methane emission in a large shallow eutrophic lake in subtropical climate. *Journal of Geophysical Research: Biogeosciences*, 122 (7), 1597-1614. <https://doi.org/10.1002/2017JG003805>
- Xing, Y. P., Xie, P., Yang, H., Ni, L. Y., Wang, Y. S., & Tang, W. H. (2004). Diel variation of methane fluxes in summer in a eutrophic subtropical lake in China. *Journal of Freshwater Ecology*, 19, 639-644. <https://doi.org/10.1080/02705060.2004.9664745>
- Xing, Y. P., Xie, P., Yang, H., Ni, L. Y., Wang, Y. S., & Rong, K. W. (2005). Methane and carbon dioxide fluxes from a shallow hypereutrophic subtropical lake in China. *Atmospheric Environment*, 39, 5532-5540. <https://doi.org/10.1016/j.atmosenv.2005.06.010>
- Xing, Y. P., Xie, P., Yang, H., Wu, A. P., & Ni, L. Y. (2006). The change of gaseous carbon fluxes following the switch of dominant producers from macrophytes to algae in a shallow subtropical lake of China. *Atmospheric Environment*, 40, 8034-8043.  
<https://doi.org/10.1016/j.atmosenv.2006.05.033>
- Yang, H. (2014). China must continue the momentum of green law. *Nature*, 509, 535-535.  
<https://doi.org/10.1038/509535a>
- Yang, H., Andersen, T., Dörsch, P., Tominaga, K., Thrane, J. -E., & Hessen, D. O. (2015a). Greenhouse gas metabolism in Nordic boreal lakes. *Biogeochemistry*, 126, 211-225.  
<https://doi.org/10.1007/s10533-015-0154-8>
- Yang, H., & Flower R. J. (2012). Potentially massive greenhouse-gas sources in proposed tropical dams. *Frontiers in Ecology and the Environment*, 10, 234-235.  
<https://doi.org/10.1890/12.WB.014>
- Yang, H., Xie, P., Ni, L. Y., & Flower, R. J. (2011). Underestimation of CH<sub>4</sub> emission from freshwater lakes in China. *Environment Science & Technology*, 45, 4203-4204.  
<https://doi.org/10.1021/es2010336>
- Yang, H., Xing, Y. P., Xie, P., Ni, L. Y., & Rong, K. W. (2008). Carbon source/sink function of a subtropical, eutrophic lake determined from an overall mass balance and a gas exchange and carbon burial balance. *Environmental Pollution*, 151, 559-568.  
<https://doi.org/10.1016/j.envpol.2007.04.006>
- Yang, P., Bastviken, D., Jin, B. S., Mou, X. J., & Tong, C. (2017a). Effects of coastal marsh conversion to shrimp aquaculture ponds on CH<sub>4</sub> and N<sub>2</sub>O emissions. *Estuarine, Coastal and Shelf Science*, 199, 125-131. <https://doi.org/10.1016/j.ecss.2017.09.023>

- Yang, P., He, Q.H., Huang, J.F., Tong, C., 2015b. Fluxes of greenhouse gases at two different aquaculture ponds in the coastal zone of southeastern China. *Atmospheric Environment*, 115, 269-277. <https://doi.org/10.1016/j.atmosenv.2015.05.067>
- Yang, P., Lai, D. Y. F., Jin, B. S., Bastviken, D., Tan, L. S., & Tong, C. (2017b). Dynamics of dissolved nutrients in the aquaculture shrimp ponds of the Min River estuary, China: Concentrations, fluxes and environmental loads. *Science of The Total Environment*, 603-604, 256-267. <https://doi.org/10.1016/j.scitotenv.2017.06.074>
- Yang, P., Zhang Y. F., Lai, D. Y. F., Tan, L. S., Jin, B. S., & Tong, C. (2018). Fluxes of carbon dioxide and methane across the water–atmosphere interface of aquaculture shrimp ponds in two subtropical estuaries: The effect of temperature, substrate, salinity and nitrate. *Science of The Total Environment*, 635, 1025-1035. <https://doi.org/10.1016/j.scitotenv.2018.04.102>
- Yang, P., Wang, M. H., Lai, D. Y. F., Chune, K. P., Huang, J. F., Wan, S. A., Bastviken, D., & Tong, C. (2019). Methane dynamics in an estuarine brackish *Cyperus malaccensis* marsh: Production and porewater concentration in soils, and net emissions to the atmosphere over five years. *Geoderma*, 337, 132-142. <https://doi.org/10.1016/j.geoderma.2018.09.019>
- Yuan, J. J., Xiang, J., Liu, D. Y., Kang, H., He, T. H., Kim, S., Lin, Y. X., Freeman, C., & Ding, W. X. (2019). Rapid growth in greenhouse gas emissions from the adoption of industrial-scale aquaculture. *Nature Climate Change*, <https://doi.org/10.1038/s41558-019-0425-9>
- Yvon-Durocher, G., Allen, A. P., Bastviken, D., Conrad, R., Gudas, C., St-Pierre, A., ThanhDuc, N., & del Giorgio, P. A. (2014). Methane fluxes show consistent temperature dependence across microbial to ecosystem scales. *Nature*, 507, 488-491.
- Zhang, L., Wang, L., Yin, K. D., Lü, Y., Zhang, D. R., Yang, Y. Q., & Huang, X. P. (2013). Pore water nutrient characteristics and the fluxes across the sediment in the Pearl River estuary and adjacent waters, China. *Estuarine, Coastal and Shelf Science*, 133, 182-192. <https://doi.org/10.1016/j.ecss.2013.08.028>
- Zhang, Y. F., Yang, P., Yang, H., Tan, L. S., Guo, Q. Q., Zhao, G. H., Li, L., Gao, Y.C., & Tong, C. (2019). Plot-scale spatiotemporal variations of CO<sub>2</sub> concentration and flux across water-air interfaces at aquaculture shrimp ponds in a subtropical estuary. *Environmental Science and Pollution Research*, <https://doi.org/10.1007/s11356-018-3929-3>
- Zhao, Y., Wu, B. F., & Zeng, Y. (2013). Spatial and temporal patterns of greenhouse gas emissions from Three Gorges Reservoir of China. *Biogeosciences*, 10, 1219-1230. <https://doi.org/10.5194/bg-10-1219-2013>
- Zhu, D., Wu, Y., Chen, H., He, Y. X., & Wu, N. (2016). Intense methane ebullition from open water area of a shallow peatland lake on the eastern Tibetan Plateau. *Science of The Total Environment*, 542, 57-64. <https://doi.org/10.1016/j.scitotenv.2015.10.087>
- Zhu, R. B., Liu, Y. S., Xu, H., Huang, T., Sun, J. J., Ma, E. D., & Sun, L. G. (2010). Carbon dioxide and methane fluxes in the littoral zones of two lakes, East Antarctica. *Atmospheric Environment*, 44, 304-311. <https://doi.org/10.1016/j.atmosenv.2009.10.038>

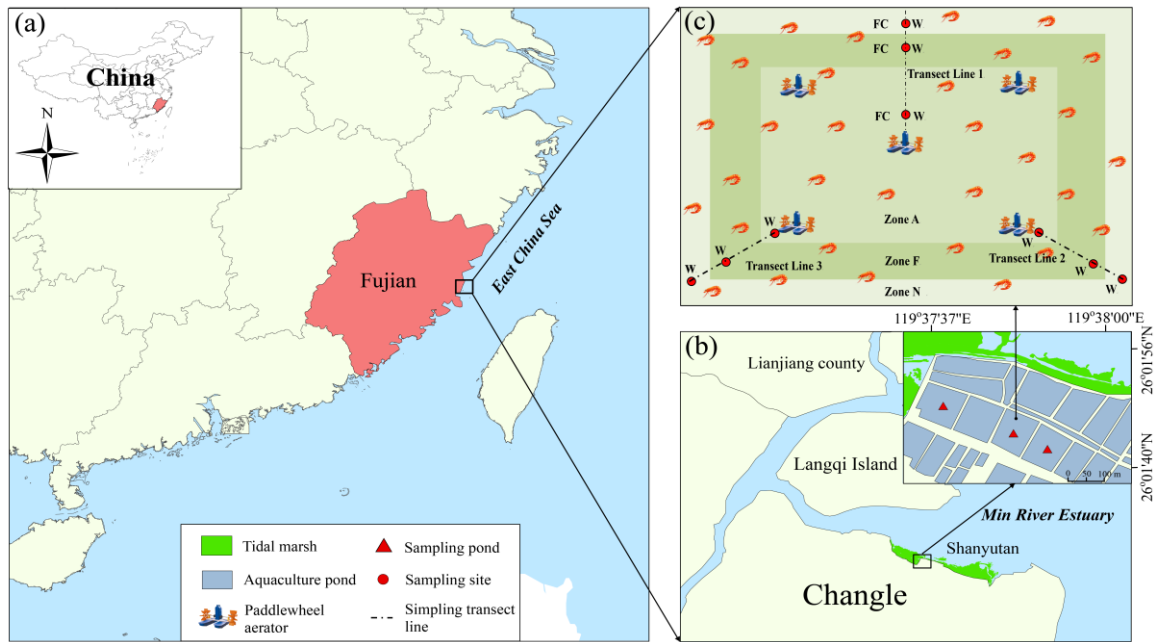


**Figure 1.** Location of the study area (a) and sampling sites (b) in Shanyutan wetland of Min River estuary. Design of aquaculture shrimp pond and the location of spatial sampling sites (red dots) (c). Zone N, F and A were nearshore area, feeding area and aeration area, respectively. W, water concentration samples; and FC, air samples collection by floating chambers.

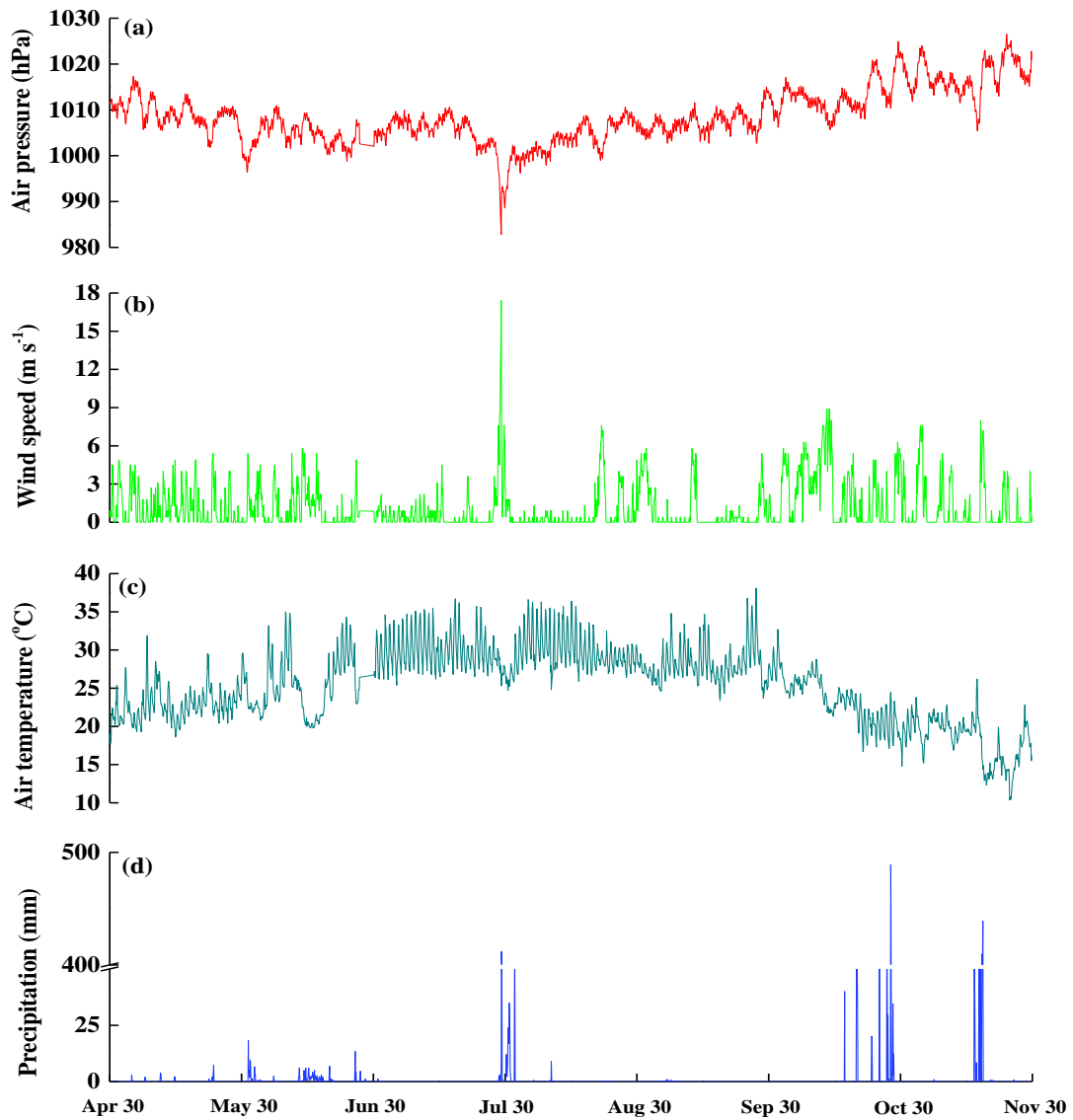


**Figure 2.** Temporal variation of the (a) air pressure, (b) wind speed, (c) air temperature, and (d) precipitation in the shrimp ponds at the Min River estuary during the aquaculture period (from June to November). Bars represent mean $\pm$ SE ( $n = 3$  ponds).

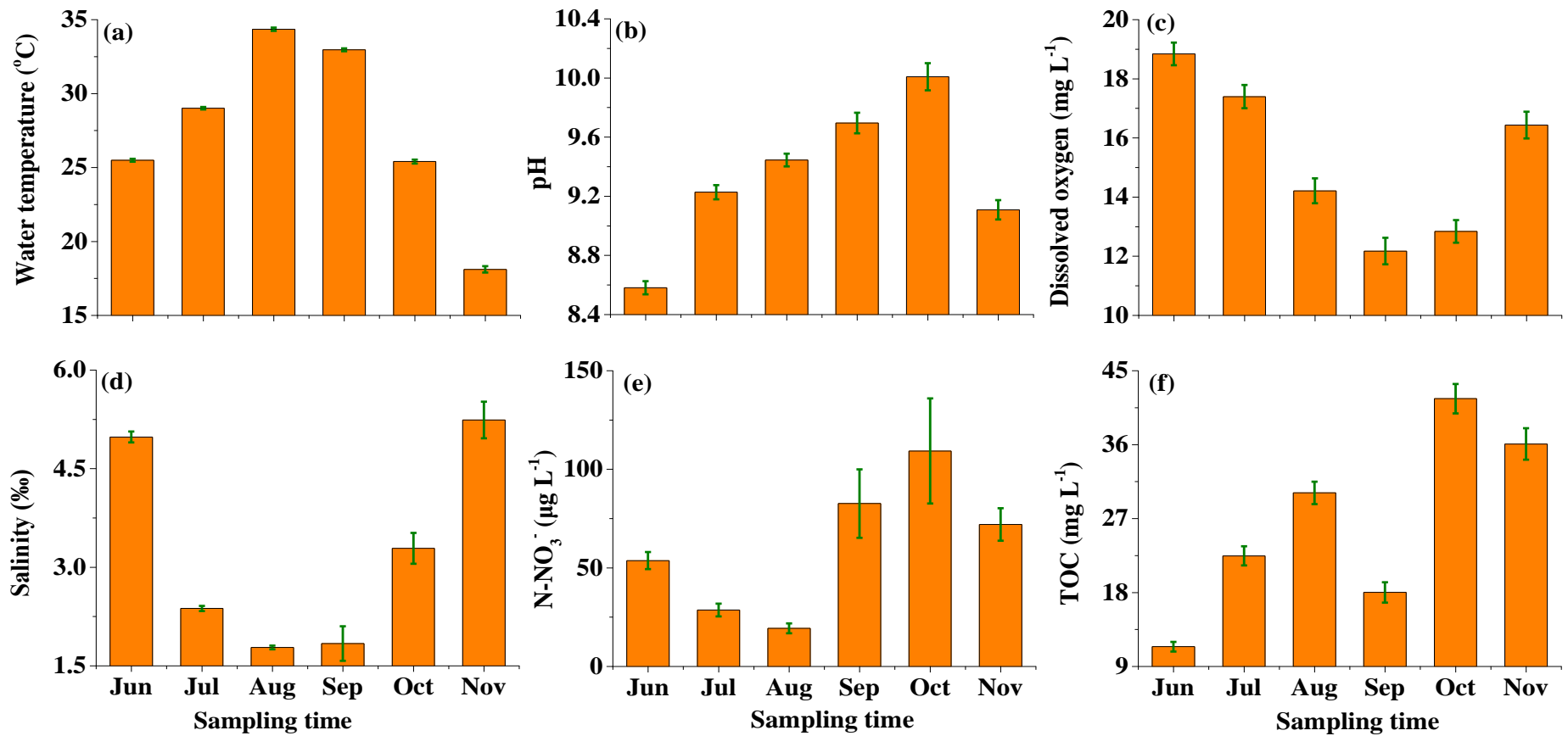
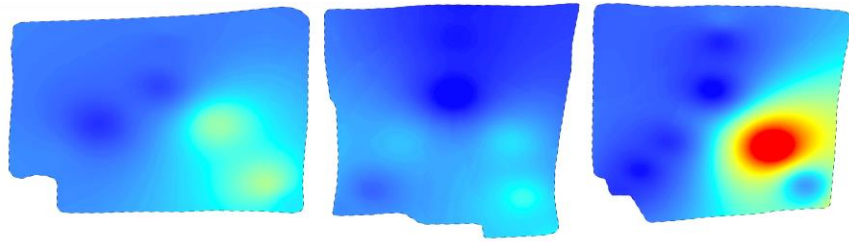
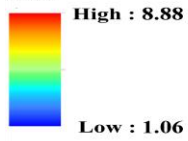


**Figure 3.** Temporal variation of (a) temperature, (b) pH, (c) dissolved oxygen (DO), (d) salinity, (e) N-NO<sub>3</sub><sup>-</sup>, and (f) total organic carbon (TOC) in the surface water (20 cm depth) of shrimp ponds at the Min River estuary during the aquaculture period (from June to November). Bars represent mean±SE ( $n = 3$  ponds).

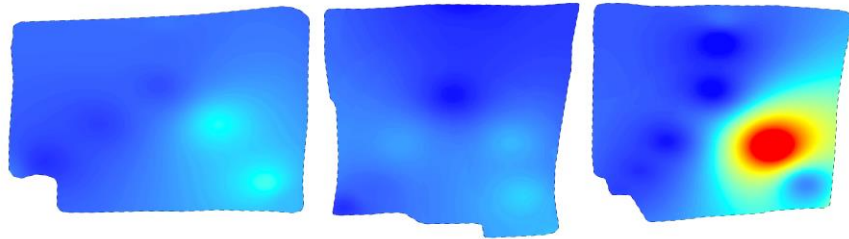
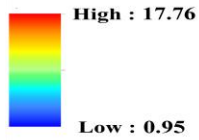
**a June**

CH<sub>4</sub> Concentrations (μM)



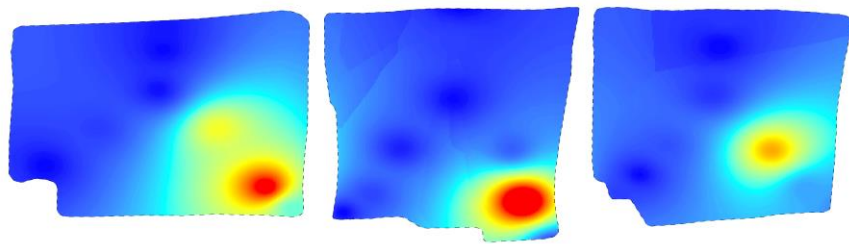
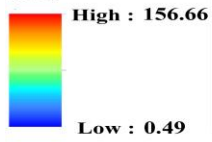
**b July**

CH<sub>4</sub> Concentrations (μM)



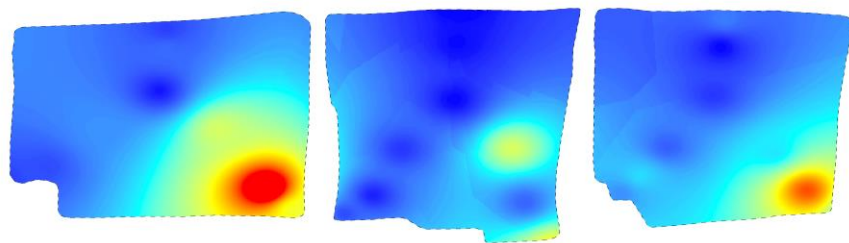
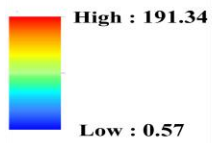
**c August**

CH<sub>4</sub> Concentrations (μM)



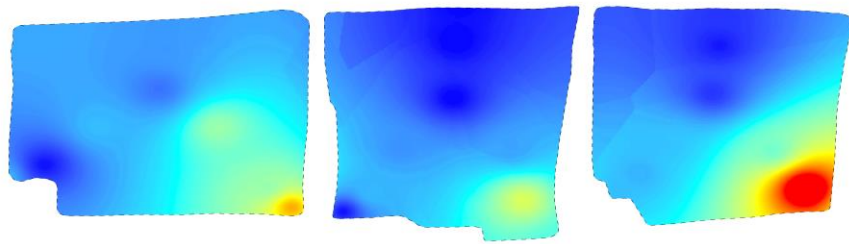
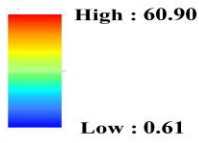
**d September**

CH<sub>4</sub> Concentrations (μM)



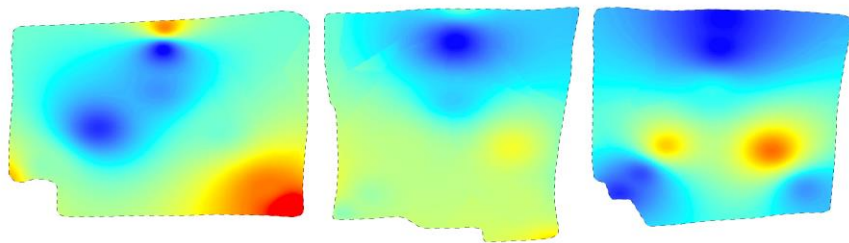
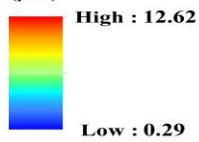
**e October**

CH<sub>4</sub> Concentrations (μM)



**f November**

CH<sub>4</sub> Concentrations (μM)



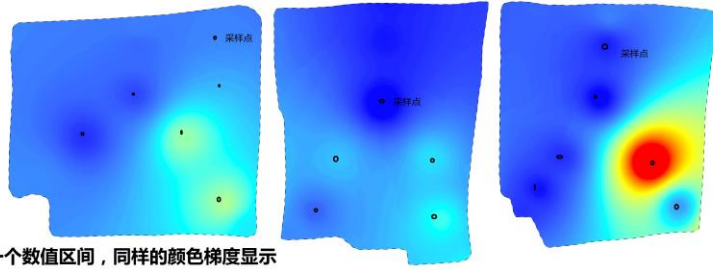
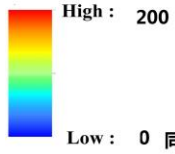
**Pond I**

**Pond II**

**Pond III**

**a June**

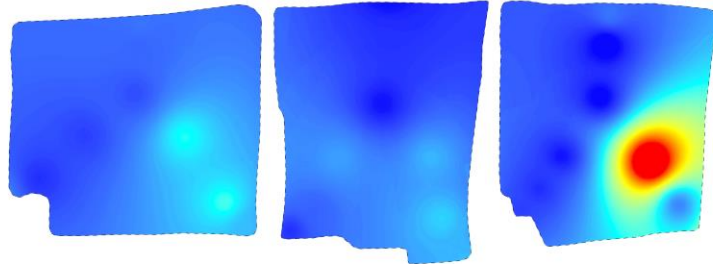
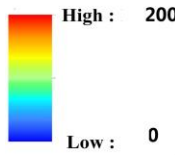
CH<sub>4</sub> Concentrations (μM)



同一个数值区间, 同样的颜色梯度显示

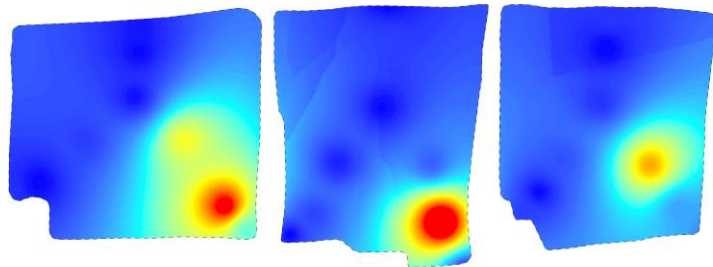
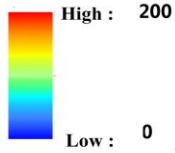
**b July**

CH<sub>4</sub> Concentrations (μM)



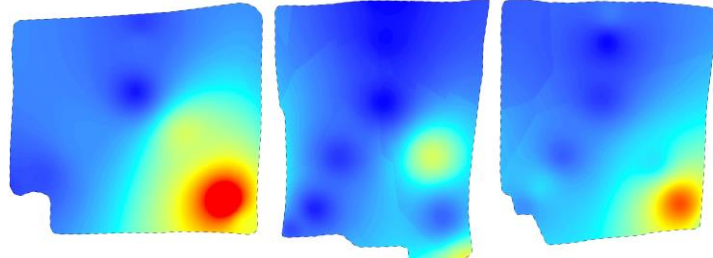
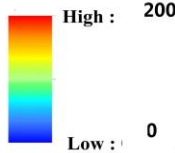
**c August**

CH<sub>4</sub> Concentrations (μM)



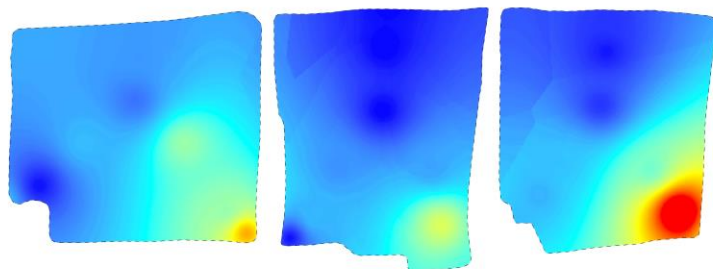
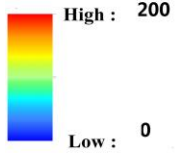
**d September**

CH<sub>4</sub> Concentrations (μM)



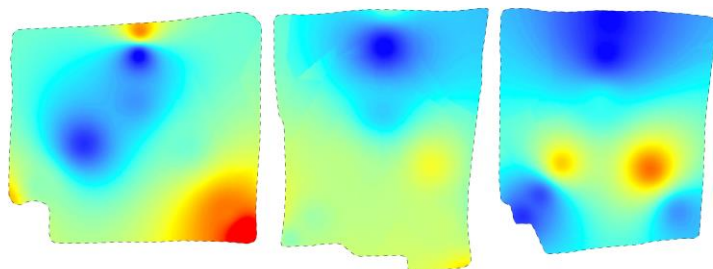
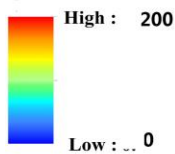
**e October**

CH<sub>4</sub> Concentrations (μM)



**f November**

CH<sub>4</sub> Concentrations (μM)



Pond I

Pond II

Pond III

**Figure 4.** Spatial variation of the CH<sub>4</sub> concentration in the surface water (20 cm depth) of shrimp ponds at the Min River estuary during the aquaculture period (from June to November).

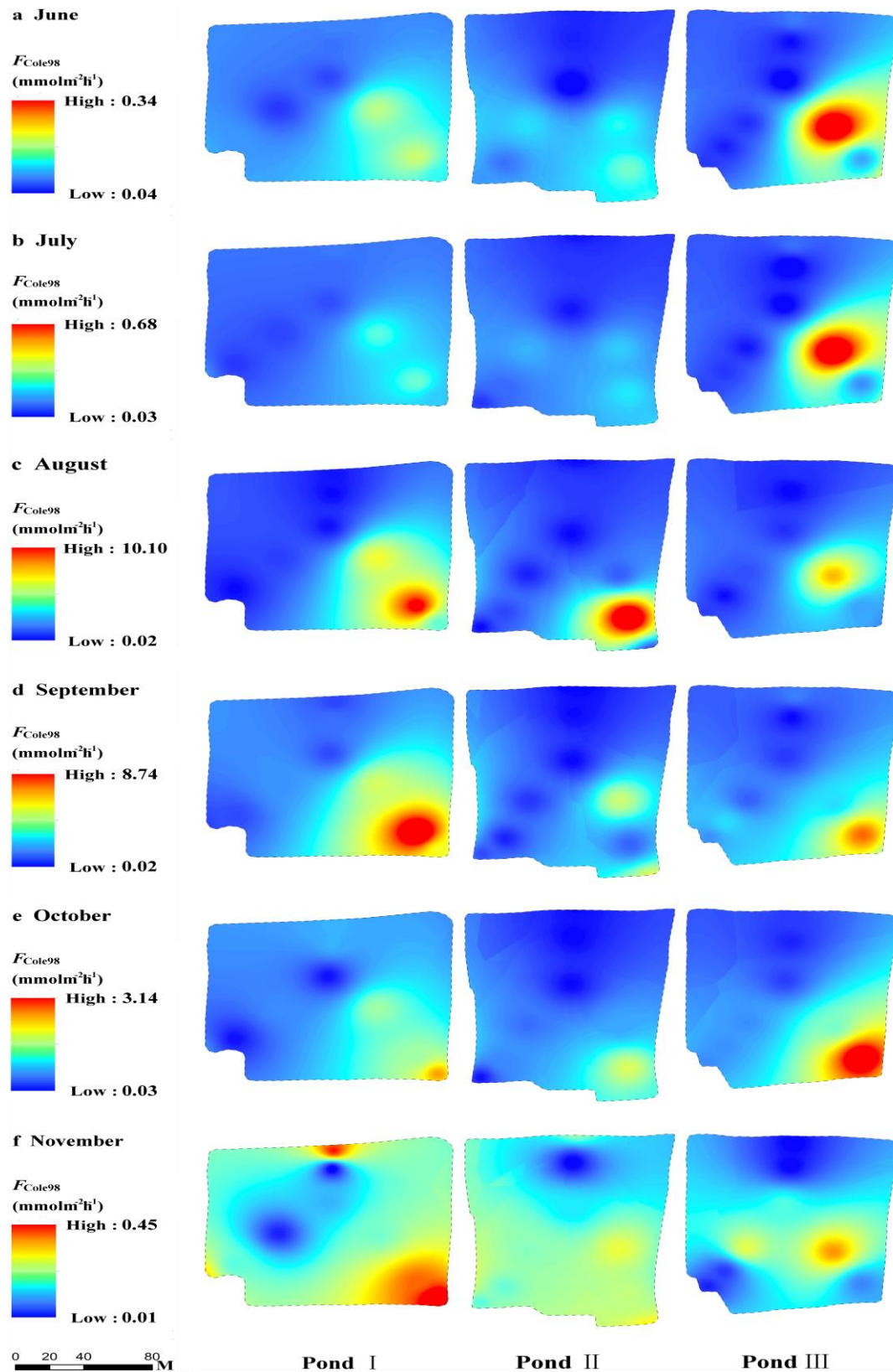


**Figure 5.** Spatial variation of the CH<sub>4</sub> diffusion flux in the surface water (20 cm depth) of shrimp ponds at the Min River estuary during the aquaculture period (from June to

November)

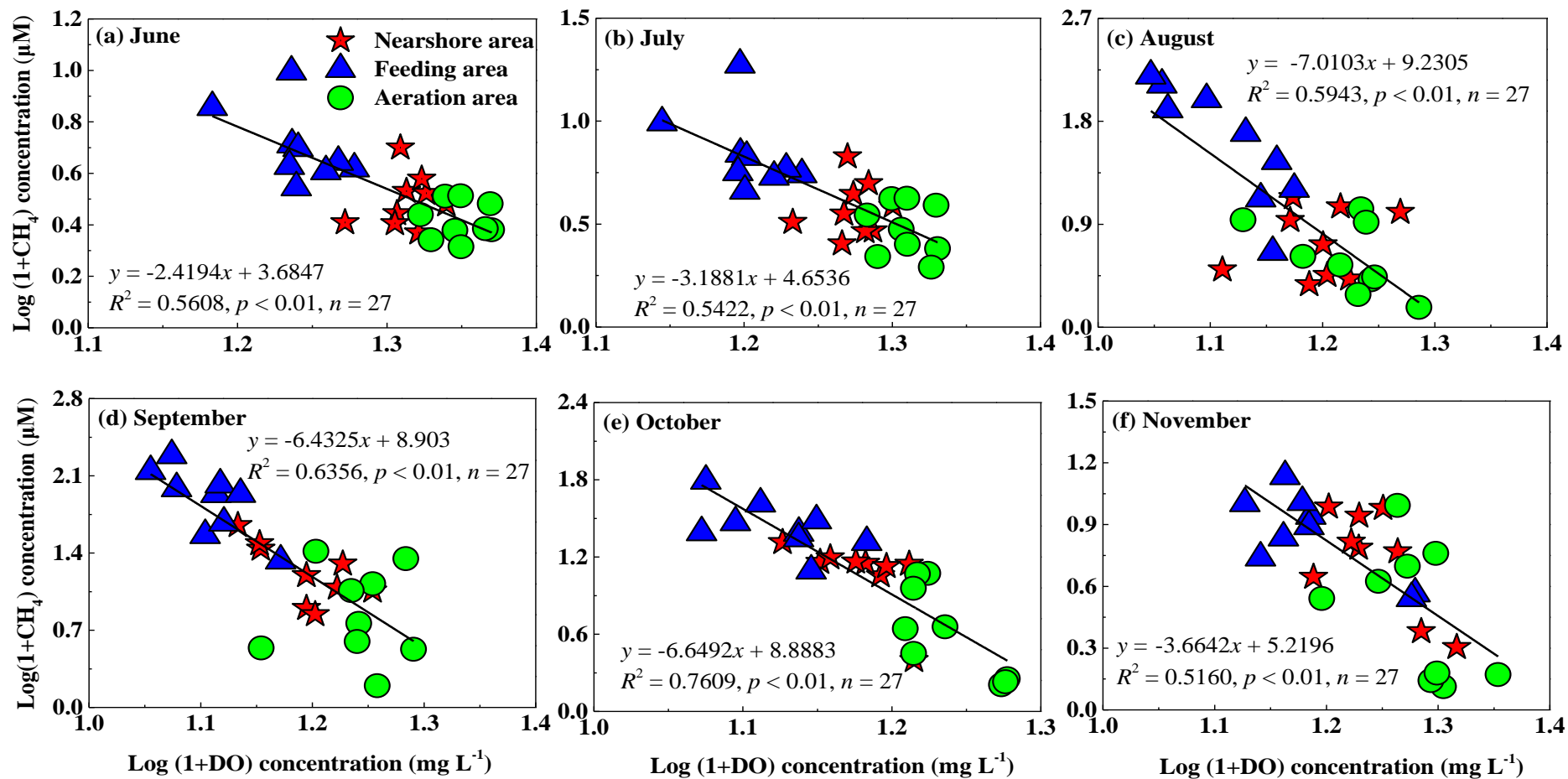


**Figure 6.** Relationship between the CH<sub>4</sub> concentrations and dissolved oxygen (DO) concentration in the surface water (20 cm depth) at shrimp ponds in the Min River estuary during each sampling campaign. Parameter bounds on the regression coefficients are 95% confidence limits.

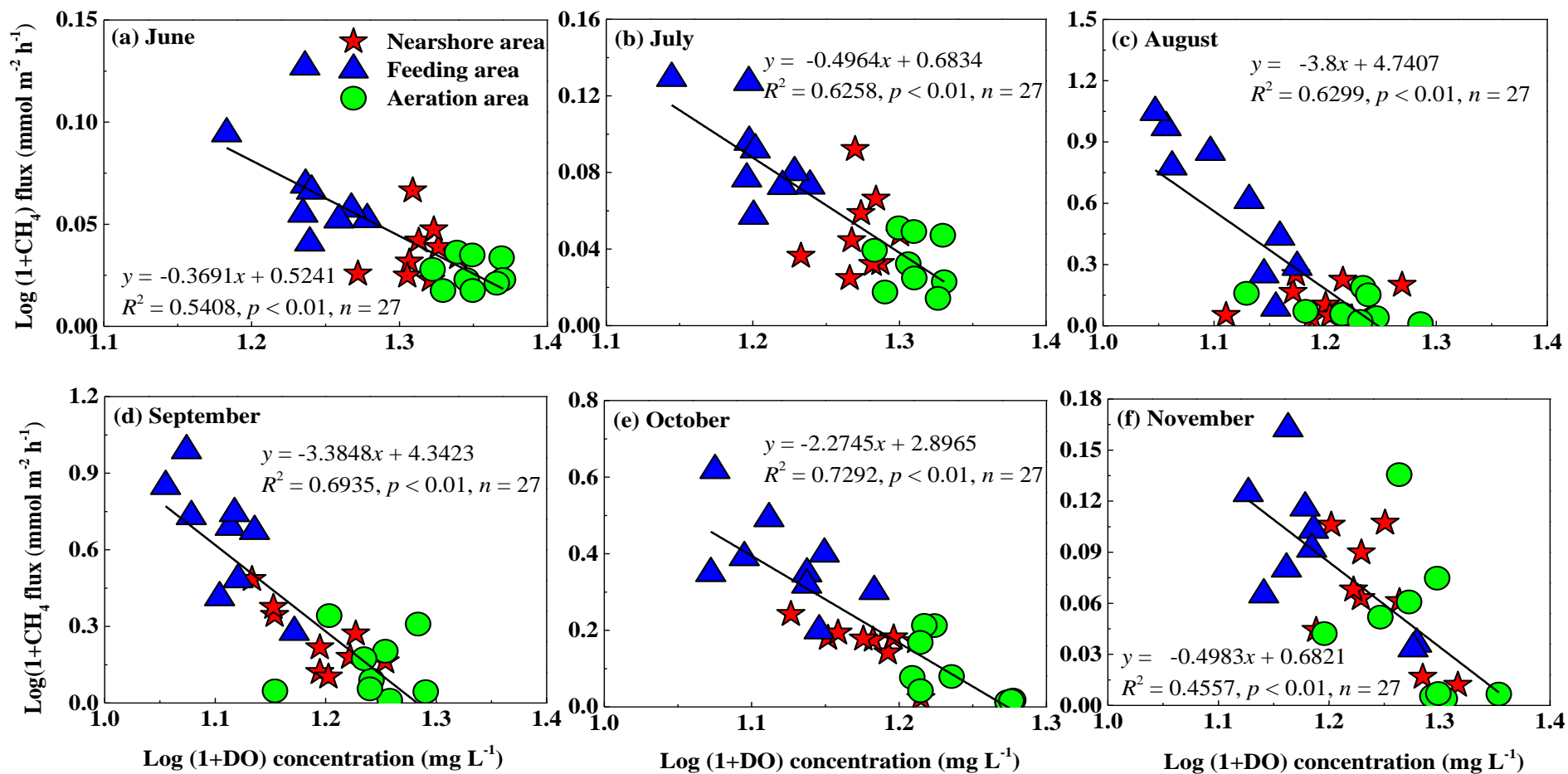


**Figure 7.** Linear relationship between  $\text{CH}_4$  diffusion flux and dissolved oxygen (DO) concentration in the surface water (20 cm depth) at shrimp ponds in the Min River estuary during each campaign. Parameter bounds on the regression coefficients are 95% confidence limits.

**Table 1.** Summary of two-way ANOVAs (with ponds ID specified as the random term) that examining the effect of sampling zones, sampling time (months) and their interactions on water CH<sub>4</sub> concentration and on CH<sub>4</sub> fluxes at the shrimp ponds in the Min River Estuary.

|                      | Water CH <sub>4</sub> concentration |                    |           |                   |                 | CH <sub>4</sub> fluxes across the water-air |                    |           |                   |                 |
|----------------------|-------------------------------------|--------------------|-----------|-------------------|-----------------|---|--------------------|-----------|-------------------|-----------------|
| <i>Fixed effect</i>  | <i>Sum of squares</i>               | <i>Mean square</i> | <i>df</i> | <i>F values</i>   | <i>P values</i> | <i>Sum of squares</i>                       | <i>Mean square</i> | <i>df</i> | <i>F values</i>   | <i>P values</i> |
| Zones                | 55.89                               | 27.946             | 2         | 69.167            | <0.001          | 126.59                                      | 63.29              | 2         | 65.281            | <0.001          |
| Months               | 45.66                               | 9.132              | 5         | 22.603            | <0.001          | 146.67                                      | 29.33              | 5         | 30.255            | <0.001          |
| Zones × Months       | 8.72                                | 0.872              | 10        | 2.159             | 0.0236          | 14.61                                       | 1.46               | 10        | 1.507             | 0.142           |
| Residuals            | 57.37                               | 0.404              | 142       |                   |                 | 137.68                                      | 0.97               | 142       |                   |                 |
| <i>Random effect</i> |                                     |                    | <i>df</i> | <i>Chi-square</i> | <i>P values</i> |   |                    | <i>df</i> | <i>Chi-square</i> | <i>P values</i> |
| Ponds                |                                     |                    | 1         | 7.680             | 0.0055          |   |                    | 1         | 7.828             | 0.0051          |

**Table 2.** Summary of linear mixed-effect models fitted for water CH<sub>4</sub> concentration and CH<sub>4</sub> fluxes across the water-air interface. Models are ranked in order of the lowest Akaike information criterion corrected for low samples sizes (AICc) along with delta AICc. The predictors of the best model with lowest AICc were tested by Type II Wald test and the significant positive (↑) or negative effects (↓) of chosen continuous predictors are indicated.

|  | AICc   | Variab                          |
|--|--------|---------------------------------|
| <b>Water CH<sub>4</sub> concentration</b>  |        |                                 |
| Air temperature+Atmospheric pressure+Water temperature+Wind speed+pH+DO+TOC+Salinity+NO <sub>3</sub> <sup>-</sup> -N | 388.94 | -Air te                         |
| Atmospheric pressure+Water temperature+Wind speed+pH+DO+TOC+Salinity+NO <sub>3</sub> <sup>-</sup> -N                 | 382.31 | -Water                          |
| Atmospheric pressure+Wind speed+pH+DO+TOC+Salinity+NO <sub>3</sub> <sup>-</sup> -N                                   | 375.89 | -Wind                           |
| Atmospheric pressure+pH+DO+TOC+Salinity+NO <sub>3</sub> <sup>-</sup> -N  | 369.75 | -TOC                            |
| Atmospheric pressure+pH+DO+Salinity+NO <sub>3</sub> <sup>-</sup> -N  | 364.51 | -NO <sub>3</sub> <sup>-</sup> - |
| Atmospheric pressure+pH+DO+Salinity  | 359.45 | -pH                             |
| Atmospheric pressure+DO+Salinity   | 358.91 |                                 |
| <i>Predictors from best model tested</i>   |        |                                 |
| DO (↓)   |        |                                 |
| Atmospheric pressure (↓)   |        |                                 |
| Salinity (↓)   |        |                                 |
| <b>CH<sub>4</sub> fluxes across the water-air</b>  |        |                                 |
| Air temperature+Atmospheric pressure+Water temperature+Wind speed+pH+DO+TOC+Salinity+NO <sub>3</sub> <sup>-</sup> -N | 519.57 | -Air te                         |
| Atmospheric pressure+Water temperature+Wind speed+pH+DO+TOC+Salinity+NO <sub>3</sub> <sup>-</sup> -N                 | 513.06 | -Wind                           |
| Atmospheric pressure+Water temperature+pH+DO+TOC+Salinity+NO <sub>3</sub> <sup>-</sup> -N                            | 506.78 | -Water                          |
| Atmospheric pressure+pH+DO+TOC+Salinity+NO <sub>3</sub> <sup>-</sup> -N  | 501.65 | -NO <sub>3</sub> <sup>-</sup> - |
| Atmospheric pressure+pH+DO+TOC+Salinity  | 495.90 | -TOC                            |
| Atmospheric pressure+pH+DO+Salinity  | 490.45 | -Salini                         |
| Atmospheric pressure+pH+DO   | 490.18 |                                 |
| <i>Predictors from best model tested</i>   |        |                                 |
| DO (↓)   |        |                                 |
| Atmospheric pressure (↓)   |        |                                 |
| pH (↑)   |        |                                 |